

## Chapter 4

# Calculation of periodic diffractive micro- and nanostructures

This chapter describes a numerical method for solving the diffraction problem in periodic diffractive micro- and nanostructures. The method is used to calculate and study the diffraction patterns for a number of modern trends in nanophotonics, including plasmonics, metamaterials, nanometrology.

Section 4.1 deals with the method of rigorous coupled-wave analysis to solve the problem of diffraction of a plane wave on two- and three-diffraction structures and diffractive gratings. This numerical method for solving Maxwell's equations is focused on the analysis of micro- and nanostructures described by a periodic function of the dielectric constant. This variant of the method is a modification of the numerically stable modification of the method of rigorous coupled-wave analysis, proposed by M.G. Moharam, D.A. Pommet, B.G. Eric and T.K. Gaylord in 1995 for solving the problem on two-dimensional diffractive structures. Attention is also given to the current variant of the method, including the case of tensor dielectric and magnetic permittivities and diffraction on three-dimensional structures. The considered variant of the method also includes the application of special rules of expansion into a Fourier series of the product of functions proposed by Lifeng Li in 1996. The application of these rules greatly improves the convergence of the method in solving the diffraction problem on metallic and metallic-dielectric diffractive structures.

Section 4.2 examines surface electromagnetic waves (surface plasmon-polaritons), with the study and calculation of the diffraction structures for the formation of interference patterns of surface electromagnetic waves. The diffractive structures consist of a dielectric diffraction grating and a metallic layer deposited on the substrate. The calculation and modelling of structures are carried out by rigorous coupled-wave analysis. The parameters of the diffraction structure are calculated from the excitation conditions at the lower boundary of the metal layer of the given set of surface electromagnetic waves of different shapes and directions. As a result, a periodic interference pattern of surface electromagnetic waves forms directly under the metallic layer. Periods of the formed interference patterns are substantially of the sub-wavelength type. The promising field of application

of the considered diffraction structures is nanolithography, based on recording the interference patterns of surface electromagnetic waves in an electron resist.

Section 4.3 considers the magneto-optical properties of two-layer metallic-dielectric heterostructures consisting of a metallic diffractive grating and a dielectric magnetized layer. Calculation and study of the magneto-optical properties of structures are based on the method of rigorous coupled-wave analysis. The results show that these structures have resonant magneto-optical effects associated with the rotation of the plane of polarization of the incident wave and with a change in the reflectance (transmittance) of the structure when the magnetization of the layer changes. The above structures can be used as magnetic field sensors, gas sensors, the devices of the intensity modulation of light, controlled by an external magnetic field.

In Section 4.4 we consider the problem of metrology of nanostructures based on the reflectometry method (ellipsometry). Optical reflectometry is a contactless method of measuring the parameters of micro- and nanostructures by measuring reflected ???from the structure of the field???. The section reviews a number of mathematical methods for determining the geometric parameters of diffraction gratings by measuring the parameters of the wave in the reflected zero order diffraction. The reflected field is by rigorous coupled-wave analysis. The effectiveness of the methods is illustrated by the example of determining the parameters of a trapezoidal profile. The error in determining the parameters of a trapezoidal profile is less than 1 nm.

## **4.1. The method of rigorous coupled-wave analysis for solving the diffraction problem in periodic diffractive structures**

This section describes the method of Fourier modes (rigorous coupled-wave analysis), designed to address the problem of diffraction of a plane electromagnetic wave on a periodic diffractive structure. This method of solving Maxwell's equations is a variation of the differential method and occupies a leading in the breadth of functionality and use. The method is applicable for the analysis of periodic structures with complex geometry, the material of the structure can be anisotropic. Using layers of an anisotropic absorbing material, the method can be used efficiently to solve the problem of diffraction on aperiodic structures [14, 15].

### ***4.1.1. The equation of a plane wave***

This item is auxiliary. We considered the conclusion of the general equation of a plane wave in an isotropic medium used in the following description of the rigorous coupled-wave analysis.

We write the Maxwell equations and constitutive equations in the Gaussian system of units:

$$\begin{cases} \nabla \times \mathbf{E} = -\frac{1}{c} \frac{\partial}{\partial t} \mathbf{B}, \\ \nabla \times \mathbf{H} = \frac{1}{c} \frac{\partial}{\partial t} \mathbf{D}, \\ \mathbf{B} = \mu \mathbf{H}, \\ \mathbf{D} = \varepsilon \mathbf{E}. \end{cases} \quad (4.1.1)$$

For a monochromatic field

$$\begin{aligned} \mathbf{E}(x, y, z, t) &= \mathbf{E}(x, y, z) \exp(-i\omega t), \\ \mathbf{H}(x, y, z, t) &= \mathbf{H}(x, y, z) \exp(-i\omega t), \end{aligned} \quad (4.1.2)$$

system (4.1.1) becomes:

$$\begin{cases} \nabla \times \mathbf{E} = ik_0 \mu \mathbf{H}, \\ \nabla \times \mathbf{H} = -ik_0 \varepsilon \mathbf{E}, \end{cases} \quad (4.1.3)$$

where  $k_0 = 2\pi/\lambda$ ,  $\lambda$  is the wavelength. Expanding the rotor operator, we obtain:

$$\nabla \times \mathbf{E} = \begin{bmatrix} \frac{\partial E_z}{\partial y} - \frac{\partial E_y}{\partial z} \\ \frac{\partial E_x}{\partial z} - \frac{\partial E_z}{\partial x} \\ \frac{\partial E_y}{\partial x} - \frac{\partial E_x}{\partial y} \end{bmatrix} = ik_0 \mu \begin{bmatrix} H_x \\ H_y \\ H_z \end{bmatrix}, \quad \nabla \times \mathbf{H} = \begin{bmatrix} \frac{\partial H_z}{\partial y} - \frac{\partial H_y}{\partial z} \\ \frac{\partial H_x}{\partial z} - \frac{\partial H_z}{\partial x} \\ \frac{\partial H_y}{\partial x} - \frac{\partial H_x}{\partial y} \end{bmatrix} = -ik_0 \varepsilon \begin{bmatrix} E_x \\ E_y \\ E_z \end{bmatrix}. \quad (4.1.4)$$

To obtain the equation of a plane wave we seek the solution of equations (4.1.4) in the form of

$$\Phi(x, y, z) = \Phi \exp(ik_0(\alpha x + \beta y + \gamma z)), \quad (4.1.5)$$

where  $\Phi = [E_x \ E_y \ E_z \ H_x \ H_y \ H_z]^T$  is the column vector of the field components. The values  $\alpha, \beta, \gamma$  in (4.1.5) determine the direction of propagation of a plane wave. Substituting (4.1.5) into (4.1.4), we obtain:

$$ik_0 \begin{bmatrix} \beta E_z - \gamma E_y \\ \gamma E_x - \alpha E_z \\ \alpha E_y - \beta E_x \end{bmatrix} = ik_0 \mu \begin{bmatrix} H_x \\ H_y \\ H_z \end{bmatrix}, \quad ik_0 \begin{bmatrix} \beta H_z - \gamma H_y \\ \gamma H_x - \alpha H_z \\ \alpha H_y - \beta H_x \end{bmatrix} = -ik_0 \varepsilon \begin{bmatrix} E_x \\ E_y \\ E_z \end{bmatrix}. \quad (4.1.6)$$

We represent the equation (4.1.6) in matrix form:

$$\begin{bmatrix} 0 & -\gamma & \beta & -\mu & 0 & 0 \\ \gamma & 0 & -\alpha & 0 & -\mu & 0 \\ -\beta & \alpha & 0 & 0 & 0 & -\mu \\ \varepsilon & 0 & 0 & 0 & -\gamma & \beta \\ 0 & \varepsilon & 0 & \gamma & 0 & -\alpha \\ 0 & 0 & \varepsilon & -\beta & \alpha & 0 \end{bmatrix} \Phi = \mathbf{A} \cdot \Phi = \mathbf{0}. \quad (4.1.7)$$

By direct computation we can easily obtain that the determinant of system (4.1.7) has the form:

$$\det \mathbf{A} = \varepsilon \mu (\alpha^2 + \beta^2 + \gamma^2 - \varepsilon \mu)^2. \quad (4.1.8)$$

The sought non-trivial solution of (4.1.7) exists when the determinant (4.1.8) is zero. In the case  $\mu = 1$  the determinant (4.1.8) vanishes if

$$\alpha^2 + \beta^2 + \gamma^2 = \varepsilon. \quad (4.1.9)$$

Let us write the solution of (4.1.6) explicitly. Under the condition (4.1.9), the rank of the system (4.1.7) is equal to four, so to record the solution we fix the values of the amplitudes  $E_z$  and  $H_z$ . We introduce the so-called E- and H-waves. For the E-wave  $E_z \neq 0$ ,  $H_z \equiv 0$  and for the H-wave  $H_z \equiv 0$ ,  $E_z \equiv 0$ . We represent the desired solution as a superposition of the E- and H-waves in the form:

$$\Phi = \frac{1}{\sqrt{\alpha^2 + \beta^2}} \begin{bmatrix} -\alpha\gamma \\ -\beta\gamma \\ \alpha^2 + \beta^2 \\ \beta\varepsilon \\ -\alpha\varepsilon \\ 0 \end{bmatrix} A'_E + \frac{1}{\sqrt{\alpha^2 + \beta^2}} \begin{bmatrix} -\beta \\ \alpha \\ 0 \\ -\alpha\gamma \\ -\beta\gamma \\ \alpha^2 + \beta^2 \end{bmatrix} A'_H, \quad (4.1.10)$$

where  $A'_E$  and  $A'_H$  are the amplitudes of the E- and H-waves, respectively.

We write the components of the vector  $\mathbf{p} = (\alpha, \beta, \gamma)$  representing the direction of the wave, in terms of angles  $\theta$  and  $\phi$  of the spherical coordinate system:

$$\alpha = \sqrt{\varepsilon} \cos\phi \sin\theta, \quad \beta = \sqrt{\varepsilon} \sin\phi \sin\theta, \quad \gamma = \sqrt{\varepsilon} \cos\theta, \quad (4.1.11)$$

where  $\theta$  is the angle between the vector  $\mathbf{p}$  and the axis  $Oz$ ,  $\phi$  is the angle between the plane of incidence and the plane  $xOz$ . For these angles, the following relations:

$$\sqrt{\alpha^2 + \beta^2} = \sqrt{\varepsilon} \sin\theta, \quad \frac{\alpha}{\sqrt{\alpha^2 + \beta^2}} = \cos\phi, \quad \frac{\beta}{\sqrt{\alpha^2 + \beta^2}} = \sin\phi. \quad (4.1.12)$$

We write separately the y- and x-components of the electric and magnetic fields:

$$\begin{aligned}
\bar{\Phi} = \begin{bmatrix} E_y \\ E_x \\ H_y \\ H_x \end{bmatrix} &= \begin{bmatrix} -\sqrt{\varepsilon} \cos \theta \sin \phi \\ -\sqrt{\varepsilon} \cos \theta \cos \phi \\ -\varepsilon \cos \phi \\ \varepsilon \sin \phi \end{bmatrix} A'_E + \begin{bmatrix} \cos \phi \\ -\sin \phi \\ -\sqrt{\varepsilon} \cos \theta \sin \phi \\ -\sqrt{\varepsilon} \cos \theta \cos \phi \end{bmatrix} A'_H = \\
&= \begin{bmatrix} \mathbf{R} & 0 \\ 0 & \mathbf{R} \end{bmatrix} \begin{bmatrix} 0 & 1 \\ -\gamma & 0 \\ -\varepsilon & 0 \\ 0 & -\gamma \end{bmatrix} \begin{bmatrix} A'_E \\ A'_H \end{bmatrix}, \quad (4.1.13)
\end{aligned}$$

where  $\mathbf{R}$  is the rotation matrix of the form:

$$\mathbf{R} = \begin{bmatrix} \cos \phi & \sin \phi \\ -\sin \phi & \cos \phi \end{bmatrix}. \quad (4.1.14)$$

To describe the polarization of the wave, we introduce an angle  $\psi$  – the angle between the vector  $\mathbf{E}$  and the plane of incidence. By the plane of incidence we mean the plane containing the vector of direction of the wave  $\mathbf{p}$  and the axis  $Oz$ . In this case,

$$A'_H = A \sin \psi, \quad A'_E = A \cos \psi. \quad (4.1.15)$$

Note that in solving the problem of diffraction the case  $\phi = 0$  corresponds to the so-called flat incidence. In this case, the  $E$ -waves are called waves with TM-polarization, and the  $H$ -waves – waves with TE-polarization.

To characterize the energy carried by the wave, it is convenient to normalize the coefficients  $A'_E$  and  $A'_H$ . We compute the  $z$ -component of the Poynting vector corresponding to the energy flux through the plane  $xOy$ . For the  $E$ -wave

$$S_z = |E_x H_y - E_y H_x| = |A'_E|^2 |\varepsilon \gamma| = |A'_E|^2 |\varepsilon \sqrt{\varepsilon}| \cos \theta, \quad (4.1.16)$$

for the  $H$ -wave

$$S_z = |E_x H_y - E_y H_x| = |A'_H|^2 |\gamma| = |A'_H|^2 |\sqrt{\varepsilon}| \cos \theta. \quad (4.1.17)$$

We redefine the expressions for the amplitudes in the form of:

$$A'_E = \frac{1}{\sqrt{|\varepsilon \sqrt{\varepsilon}| \cos \theta}} A_E, \quad (4.1.18)$$

$$A'_H = \frac{1}{\sqrt{|\sqrt{\varepsilon}| \cos \theta}} A_H. \quad (4.1.19)$$

In this case, the values  $|A_E|^2$  and  $|A_H|^2$  correspond to the energy flux through the plane  $xOy$ . Such a normalization is useful for monitoring the law of conservation of energy in solving the problem of diffraction on diffraction structures of a non-absorbing material.

### 4.1.2. The method of rigorous coupled-wave analysis in the two-dimensional case

The method of rigorous coupled-wave analysis used to solve the problem of diffraction on periodic diffraction structures consisting of a set of layers [1–13]. In each layer, the dielectric and magnetic permeabilities of materials of the structure are constant in the direction normal to the layer (along the axis  $Oz$ ). The method is based on the representation of the field in the layers of the structure in the form of segments of Fourier series and on subsequent equating of the tangential field components at the boundaries between the layers. This reduces the solution of the problem to solving a system of linear equations [1–13].

In this section we consider the method for two-dimensional gratings. In the two-dimensional case, the material properties of the structure are constant along the axis  $Oy$ . The materials of the structure are given in general terms by the tensors of dielectric permittivity and magnetic permeability.

#### 4.1.2.1 The geometry of the structure and formulation of the problem

Let us consider a grating with a period  $\Lambda$  along the axis (Fig. 4.1.1). For gratings with a continuous profile (dashed line in Fig. 4.1.1.) the method assumes the approximation of the profile of the grating by a set of binary layers. We assume that the diffractive grating consists of  $L$  binary layers (Fig. 4.1.1). The dielectric permittivity  $\varepsilon$  and magnetic permeability  $\mu$  of the layers depend only on the variable  $x$ . The boundaries of the layers are the lines  $z = d_i$ , the  $i$ -th layer is located in the range  $d_i < z < d_{i-1}$ .

Above this structure in the range  $z > d_0 = 0$  there is a homogeneous dielectric with a refractive index  $n_1 = \sqrt{\varepsilon_1}$ . Under the structure at  $z < d_L$  there is a homogeneous dielectric with a refractive index  $n_2 = \sqrt{\varepsilon_2}$ .

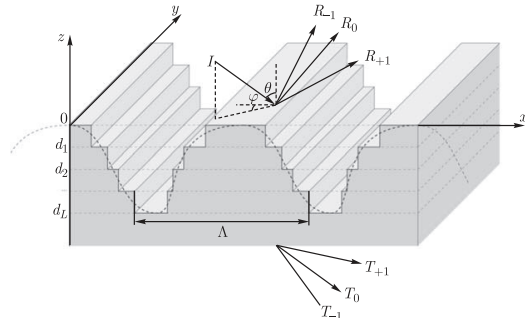


Fig. 4.1.1. Geometry of the problem of diffraction on a two-dimensional grating.

On top of the grating there is a plane monochromatic wave (wavelength  $\lambda$ ), whose direction is given by the angles  $\theta$  and  $\phi$  in a spherical coordinate system (Fig. 4.1.1). The polarization of the wave is determined by the angle  $\psi$  between the plane of incidence and the vector  $\mathbf{E}$  (see (4.1.15)).

The solution to the problem of diffraction of light on a periodic structure is to calculate the intensity or complex amplitudes of the diffraction orders. Diffraction orders are the reflected and transmitted plane waves arising from the diffraction of the incident wave on the structure. There are reflected orders with amplitudes  $R_i$ ,  $i = 0, \pm 1, \pm 2, \dots$  and transmitted orders with amplitudes  $T_i$ ,  $i = 0, \pm 1, \pm 2, \dots$  (Fig. 4.1.1). The diffraction orders are also separated into damped and propagating. The amplitude of the damped orders decreases exponentially with distance from the grating.

#### 4.1.2.2. Presentation of the field above and below the structure

The field above and below the structure is written as a superposition of plane waves (Rayleigh expansion). According to (4.1.5), (4.1.10), we represent the plane wave by the vector of six components:

$$\Phi = \begin{bmatrix} E_x & E_y & E_z & H_x & H_y & H_z \end{bmatrix}^T. \quad (4.1.20)$$

The incident wave equation has the form:

$$\Phi^I(x, y, z) = \Phi^I(\psi) \exp(i(k_{x,0}x + k_y y - k_{z,I,0}z)), \quad (4.1.21)$$

*CORRECT*  
where notation  $\Phi^I(\psi)$  indicates the dependence of the incident wave on polarization (see (4.1.15)). Constants  $k_{x,0} = k_0 n_1 \sin\theta \cos\phi$ ,  $k_y = k_0 n_1 \sin\theta \sin\phi$ ,  $k_{z,I,0} = \sqrt{(k_0 n_1)^2 - k_{x,0}^2 - k_y^2}$  in (4.1.21) are defined by the angles  $\theta$  and  $\phi$  representing the directions of the waves.

The field above the grid corresponds to a superposition of the incident wave and the reflected diffraction orders:

$$\Phi^1(x, y, z) = \Phi^I(x, y, z) + \sum_i \Phi_i^R(R_i) \exp(i(k_{x,i}x + k_y y + k_{z,I,i}z)), \quad (4.1.22)$$

where  $\Phi(R) = \Phi_E R_E + \Phi_H R_H$ . The expression for  $\Phi(R)$  corresponds to the representation (4.1.10) of the reflected wave as the sum of  $E$ - and  $H$ -waves with complex amplitudes  $R_E$  and  $R_H$ , respectively.

The field below the grating can be written similarly, in the form of a superposition of transmitted waves (diffraction orders):

$$\Phi^2(x, y, z) = \sum_i \Phi_i^T(T_i) \exp(i(k_{x,i}x + k_y y - k_{z,II,i}(z - d_L))). \quad (4.1.23)$$

Directions of orders in (4.1.22), (4.1.23) are given by the values  $k_{x,l}$ ,  $k_y$ ,  $k_{z,l}$ ,  $k_{z,ll}$  that are called propagation constants and have the form:

$$\begin{aligned} k_{x,i} &= k_0 \left( n_1 \sin \theta \cos \phi + i \frac{\lambda}{\Lambda} \right), \\ k_y &= k_0 n_1 \sin \theta \sin \phi, \\ k_{z,l,i} &= \sqrt{(k_0 n_l)^2 - k_{x,i}^2 - k_y^2}, \end{aligned} \quad (4.1.24)$$

where the index  $l$  is taken to be unity for the field over the grating and 2 – for the field under it. The submitted expression for  $k_{x,i}$  follows from the Bloch–Floquet theorem [16, 17]. From a physical point of view the form of  $k_{x,i}$  ensures that the so-called quasi-periodicity conditions

$$\Phi^l(x + \Lambda, y, z) = \Phi^l(x, y, z) \exp(ik_{x,0}\Lambda), \quad l = 1, 2. \quad (4.1.25)$$

is fulfilled.

According to (4.1.25), the amplitude of the field does not change with the shift in the period. The waves with real  $k_{z,l,i}$  are propagating, with imaginary – damped.

#### 4.1.2.3. The system of differential equations to describe the field inside the layer

Let us now consider the field inside the single  $l$ -th layer. For simplicity, we omit the index  $l$ .

The field in each layer is described by the basic Maxwell equations for a monochromatic field in the form of:

$$\begin{cases} \nabla \times \mathbf{E} = ik_0 \bar{\boldsymbol{\mu}} \mathbf{H}, \\ \nabla \times \mathbf{H} = -ik_0 \bar{\boldsymbol{\epsilon}} \mathbf{E}, \end{cases} \quad (4.1.26)$$

where  $\bar{\boldsymbol{\epsilon}}, \bar{\boldsymbol{\mu}}$  in general are tensors:

$$\bar{\boldsymbol{\epsilon}} = \begin{bmatrix} \epsilon_{1,1} & \epsilon_{1,2} & \epsilon_{1,3} \\ \epsilon_{2,1} & \epsilon_{2,2} & \epsilon_{2,3} \\ \epsilon_{3,1} & \epsilon_{3,2} & \epsilon_{3,3} \end{bmatrix}, \quad \bar{\boldsymbol{\mu}} = \begin{bmatrix} \mu_{1,1} & \mu_{1,2} & \mu_{1,3} \\ \mu_{2,1} & \mu_{2,2} & \mu_{2,3} \\ \mu_{3,1} & \mu_{3,2} & \mu_{3,3} \end{bmatrix}. \quad (4.1.27)$$

The tensor components depend only on the coordinate  $x$ . Expanding the operator of the rotor (4.1.26), we obtain:

$$\left\{ \begin{array}{l}
\frac{\partial E_z}{\partial y} - \frac{\partial E_y}{\partial z} = ik_0(\mu_{1,1}H_x + \mu_{1,2}H_y + \mu_{1,3}H_z), \\
\frac{\partial E_x}{\partial z} - \frac{\partial E_z}{\partial x} = ik_0(\mu_{2,1}H_x + \mu_{2,2}H_y + \mu_{2,3}H_z), \\
\frac{\partial E_y}{\partial x} - \frac{\partial E_x}{\partial y} = ik_0(\mu_{3,1}H_x + \mu_{3,2}H_y + \mu_{3,3}H_z), \\
\frac{\partial H_z}{\partial y} - \frac{\partial H_y}{\partial z} = -ik_0(\varepsilon_{1,1}E_x + \varepsilon_{1,2}E_y + \varepsilon_{1,3}E_z), \\
\frac{\partial H_x}{\partial z} - \frac{\partial H_z}{\partial x} = -ik_0(\varepsilon_{2,1}E_x + \varepsilon_{2,2}E_y + \varepsilon_{2,3}E_z), \\
\frac{\partial H_y}{\partial x} - \frac{\partial H_x}{\partial y} = -ik_0(\varepsilon_{3,1}E_x + \varepsilon_{3,2}E_y + \varepsilon_{3,3}E_z).
\end{array} \right. \quad (4.1.28)$$

We represent the components of the electric and magnetic fields in the form of Fourier series in the variable  $x$ :

$$\left\{ \begin{array}{l}
E_x = \sum_j S_{x,j}(z) \exp(i(k_{x,j}x + k_y y)), \\
E_y = \sum_j S_{y,j}(z) \exp(i(k_{x,j}x + k_y y)), \\
E_z = \sum_j S_{z,j}(z) \exp(i(k_{x,j}x + k_y y)), \\
H_x = -i \sum_j U_{x,j}(z) \exp(i(k_{x,j}x + k_y y)), \\
H_y = -i \sum_j U_{y,j}(z) \exp(i(k_{x,j}x + k_y y)), \\
H_z = -i \sum_j U_{z,j}(z) \exp(i(k_{x,j}x + k_y y)).
\end{array} \right. \quad (4.1.29)$$

Representations (4.1.29) are written taking into account quasi-periodic components of the variable  $x$ . We confine ourselves to the finite number of terms in the expansions (4.1.29) correspond to  $-N \leq j \leq N$ . We form from the quantities  $S_{x,j}$ ,  $S_{y,j}$ ,  $S_{z,j}$ ,  $U_{x,j}$ ,  $U_{y,j}$ ,  $U_{z,j}$  column vectors  $\mathbf{S}_x$ ,  $\mathbf{S}_y$ ,  $\mathbf{S}_z$ ,  $\mathbf{U}_x$ ,  $\mathbf{U}_y$ ,  $\mathbf{U}_z$  containing  $2N+1$  elements.

Consider the Fourier series expansion of the product of two functions  $???\varepsilon_a(x) E_b(x,y,z)???$ :

$$\begin{aligned}
\varepsilon_a(x)E_b(x) &= \left( \sum_m e_{a,m} \exp\left(i \frac{2\pi}{\Lambda} m x\right) \right) \cdot \left( \sum_l S_{b,l}(z) \exp\left(i(k_{x,l}x + k_y y)\right) \right) = \\
&= \sum_{j=l+m} \left( \sum_l e_{a,j-l} S_{b,l}(z) \right) \exp\left(i(k_{x,j}x + k_y y)\right). \tag{4.1.30}
\end{aligned}$$

We restrict ourselves in (1.4.30) by a finite number of terms in the expansion at  $-N \leq j \leq N$  and in the following expression:

$$[\varepsilon_a(x)E_b(x)] = \llbracket \varepsilon_a(x) \rrbracket \mathbf{S}_b = \llbracket \varepsilon_a(x) \rrbracket [E_b(x)], \tag{4.1.31}$$

where the square brackets denote the vector consisting of the Fourier coefficients of the expansion of the  $\varepsilon_a(x)E_b(x)$  and  $E_b(x)$  functions, and  $\llbracket \varepsilon_a(x) \rrbracket$  – the Toeplitz matrix of the Fourier coefficients, which has the following form:

$$\mathbf{Q} = \begin{bmatrix} e_0 & e_1 & e_2 & \cdots & \cdots & e_{2N} \\ e_{-1} & e_0 & e_1 & e_2 & \ddots & e_{2N-1} \\ e_{-2} & e_{-1} & e_0 & e_1 & \ddots & \vdots \\ \vdots & e_{-2} & e_{-1} & \ddots & \ddots & \vdots \\ \vdots & \ddots & \ddots & \ddots & \ddots & e_1 \\ e_{-2N} & e_{1-2N} & \cdots & \cdots & e_{-1} & e_0 \end{bmatrix}. \tag{4.1.32}$$

Substituting (4.1.29) into (1.4.28) and equating the coefficients of equal Fourier harmonics, we obtain:

$$\left\{ \begin{aligned} ik_0 \mathbf{K}_y \mathbf{S}_z - \frac{d\mathbf{S}_y}{dz} &= k_0 (\mathbf{M}_{1,1} \mathbf{U}_x + \mathbf{M}_{1,2} \mathbf{U}_y + \mathbf{M}_{1,3} \mathbf{U}_z), \\ \frac{d\mathbf{S}_x}{dz} - ik_0 \mathbf{K}_x \mathbf{S}_z &= k_0 (\mathbf{M}_{2,1} \mathbf{U}_x + \mathbf{M}_{2,2} \mathbf{U}_y + \mathbf{M}_{2,3} \mathbf{U}_z), \\ ik_0 \mathbf{K}_x \mathbf{S}_y - ik_0 K_y S_x &= k_0 (\mathbf{M}_{3,1} \mathbf{U}_x + \mathbf{M}_{3,2} \mathbf{U}_y + \mathbf{M}_{3,3} \mathbf{U}_z), \\ ik_0 \mathbf{K}_y \mathbf{U}_z - \frac{d\mathbf{U}_y}{dz} &= k_0 (\mathbf{E}_{1,1} \mathbf{S}_x + \mathbf{E}_{1,2} \mathbf{S}_y + \mathbf{E}_{1,3} \mathbf{S}_z), \\ \frac{d\mathbf{U}_x}{dz} - ik_0 \mathbf{K}_x \mathbf{U}_z &= k_0 (\mathbf{E}_{2,1} \mathbf{S}_x + \mathbf{E}_{2,2} \mathbf{S}_y + \mathbf{E}_{2,3} \mathbf{S}_z), \\ ik_0 \mathbf{K}_x \mathbf{U}_y - ik_0 \mathbf{K}_y \mathbf{U}_x &= k_0 (\mathbf{E}_{3,1} \mathbf{S}_x + \mathbf{E}_{3,2} \mathbf{S}_y + \mathbf{E}_{3,3} \mathbf{S}_z), \end{aligned} \right. \tag{4.1.33}$$

where  $\mathbf{K}_x = \text{diag} \frac{k_{x,j}}{k_0}$ ,  $\mathbf{K}_y = \text{diag} \frac{k_y}{k_0}$  the diagonal matrixes, and  $\mathbf{E}_{i,j} = \llbracket \varepsilon_{i,j} \rrbracket$  and  $\mathbf{M}_{i,j} = \llbracket \mu_{i,j} \rrbracket$  is the Toeplitz matrix of the form (4.1.32), consisting of the expansion coefficients in the Fourier series of functions  $\varepsilon_{i,i}(x)$  and  $\mu_{i,j}(x)$ .

We make the change of variables  $z' = k_0 z$  and transform the system (4.1.33) to the form:

$$\begin{cases}
-\frac{dS_y}{dz'} = \mathbf{M}_{1,1}U_x + \mathbf{M}_{1,2}U_y + \mathbf{M}_{1,3}U_z - i\mathbf{K}_yS_z, \\
-\frac{dS_x}{dz'} = -\mathbf{M}_{2,1}U_x - \mathbf{M}_{2,2}U_y - \mathbf{M}_{2,3}U_z - i\mathbf{K}_xS_z, \\
\frac{dU_y}{dz'} = \mathbf{E}_{1,1}S_x + \mathbf{E}_{1,2}S_y + \mathbf{E}_{1,3}S_z - i\mathbf{K}_yU_z, \\
-\frac{dU_x}{dz'} = -\mathbf{E}_{2,1}S_x - \mathbf{E}_{2,2}S_y - \mathbf{E}_{2,3}S_z - i\mathbf{K}_xU_z, \\
\mathbf{E}_{3,3}S_z = i\mathbf{K}_xU_y - i\mathbf{K}_yU_x - \mathbf{E}_{3,1}S_x - \mathbf{E}_{3,2}S_y, \\
\mathbf{M}_{3,3}U_z = i\mathbf{K}_xS_y - i\mathbf{K}_yS_x - \mathbf{M}_{3,1}U_x - \mathbf{M}_{3,2}U_y.
\end{cases} \quad (4.1.34)$$

We rewrite the first four equations of the system in matrix form:

$$\frac{d}{dz'} \begin{bmatrix} S_y \\ S_x \\ U_y \\ U_x \end{bmatrix} = - \begin{bmatrix} \mathbf{0} & \mathbf{0} & \mathbf{M}_{1,2} & \mathbf{M}_{1,1} \\ \mathbf{0} & \mathbf{0} & -\mathbf{M}_{2,2} & -\mathbf{M}_{2,1} \\ \mathbf{E}_{1,2} & \mathbf{E}_{1,1} & \mathbf{0} & \mathbf{0} \\ -\mathbf{E}_{2,2} & -\mathbf{E}_{2,1} & \mathbf{0} & \mathbf{0} \end{bmatrix} \begin{bmatrix} S_y \\ S_x \\ U_y \\ U_x \end{bmatrix} - \begin{bmatrix} -i\mathbf{K}_y & \mathbf{M}_{1,3} \\ -i\mathbf{K}_x & -\mathbf{M}_{2,3} \\ \mathbf{E}_{1,3} & -i\mathbf{K}_y \\ -\mathbf{E}_{2,3} & -i\mathbf{K}_x \end{bmatrix} \begin{bmatrix} S_z \\ U_z \end{bmatrix}. \quad (4.1.35)$$

We express in the last two equations (1.4.34)  $S_z$  and  $U_z$ , and substitute these expressions into (1.4.35). The result is a system of linear differential equations  $x$ - and  $y$ -Fourier components of the fields:

$$\frac{d}{dz'} \begin{bmatrix} S_y \\ S_x \\ U_y \\ U_x \end{bmatrix} = \mathbf{A} \begin{bmatrix} S_y \\ S_x \\ U_y \\ U_x \end{bmatrix}, \quad (4.1.36)$$

where

$$\mathbf{A} = \mathbf{J} - \begin{bmatrix} i\mathbf{K}_y & -\mathbf{M}_{1,3} \\ i\mathbf{K}_x & \mathbf{M}_{2,3} \\ -\mathbf{E}_{1,3} & i\mathbf{K}_y \\ \mathbf{E}_{2,3} & i\mathbf{K}_x \end{bmatrix} \begin{bmatrix} \mathbf{E}_{3,3}^{-1} & \mathbf{0} \\ \mathbf{0} & \mathbf{M}_{3,3}^{-1} \end{bmatrix} \begin{bmatrix} \mathbf{E}_{3,2} & \mathbf{E}_{3,1} & -i\mathbf{K}_x & i\mathbf{K}_y \\ -i\mathbf{K}_x & i\mathbf{K}_y & \mathbf{M}_{3,2} & \mathbf{M}_{3,1} \end{bmatrix}, \quad (4.1.37)$$

where

$$\mathbf{J} = - \begin{bmatrix} \mathbf{0} & \mathbf{0} & \mathbf{M}_{1,2} & \mathbf{M}_{1,1} \\ \mathbf{0} & \mathbf{0} & -\mathbf{M}_{2,2} & -\mathbf{M}_{2,1} \\ \mathbf{E}_{1,2} & \mathbf{E}_{1,1} & \mathbf{0} & \mathbf{0} \\ -\mathbf{E}_{2,2} & -\mathbf{E}_{2,1} & \mathbf{0} & \mathbf{0} \end{bmatrix}. \quad (4.1.38)$$

Thus, we obtain a system of linear first order differential equations for the vectors  $\mathbf{S}_x, \mathbf{S}_y, \mathbf{U}_x, \mathbf{U}_y$ . Note that the matrix  $\mathbf{A}$  has the dimension  $4(2N+1) \times 4(2N+1)$ .

*Correct rules of Fourier-expansion of the product of functions*

Formulation of the system of differential equations (4.1.36) was founded on the notion in (4.1.28) of the components of electromagnetic fields and the components of the tensor of dielectric and magnetic permeability in the form of segments of Fourier series. Fourier series representation of products of functions in (1.4.28) has its own peculiarities. The formulas (1.4.30)–(1.4.32) are of limited use.

Consider two periodic functions

$$f(x) = \sum_m f_m \exp(iKmx), \quad g(x) = \sum_m g_m \exp(iKmx), \quad K = \frac{2\pi}{\Lambda} \quad (4.1.39)$$

and the Fourier series expansion of their product

$$h(x) = f(x)g(x) = \sum_m h_m \exp(iKmx). \quad (4.1.40)$$

As a product of the Fourier coefficients of the standard values we use

$$h_j = \sum_{m=-N}^N f_{j-m} g_m, \quad (4.1.41)$$

obtained by direct multiplication of the series (4.1.39), (1.4.40). Equation (1.4.41) to compute the Fourier coefficients of the rule is called the Laurent rule. In matrix notation (1.4.41) can be written as [5]

$$[h] = [[f]][g], \quad (4.1.42)$$

where, as in (1.4.31), the square brackets denote the vectors consisting of Fourier coefficients of expansion of functions, and  $[[f]]$  is the Toeplitz matrix of the Fourier coefficients.

As shown in [5, 6], the use of (1.4.42) is correct if there are no values of  $x$  for which the functions  $f(x)$  and  $g(x)$  become discontinuous at the same time. Using the Laurent rules (1.4.42) for the product of functions with coincident points of discontinuity leads to disruption of the convergence of Fourier series at the points of discontinuity.

If the functions  $f(x)$  and  $g(x)$  are discontinuous at the same time, but the function  $h(x) = f(x)g(x)$  is continuous, it is correct to use of the so-called inverse Laurent rule [5]

$$[h] = \left[ \left[ \frac{1}{f} \right] \right]^{-1} [g]. \quad (4.1.43)$$

In the products  $\mu_{i,1}(x) \cdot H_x(x, y, z)$  and  $\varepsilon_{i,1}(x) \cdot E_x(x, y, z)$  in (4.1.28) both decomposed functions have discontinuities at the same points  $x$  corresponding to the vertical

boundaries of the media in the layers. Accordingly, the use of the Laurent rules (4.1.30)–(4.1.32) when writing (4.1.33) is erroneous. Errors in the use of the Laurent are large when working with diffraction gratings of conductive materials. In particular, the erroneous use of the Laurent rule leads to slow convergence of solutions for binary metal gratings for the case of TM-polarization [5–10]. Convergence in this case refers to the stabilization of the results of calculation of the amplitudes of the diffraction orders with increasing number of Fourier harmonics  $N$  in the representation of the field components (4.1.29).

Continuous components at the vertical boundaries of the media are the tangential components  $E_y$ ,  $E_z$ ,  $H_y$ ,  $H_z$  and normal components of electric displacement and magnetic induction  $D_x$ ,  $B_x$ . We express the discontinuous components by the continuous field components

$$\begin{aligned} E_x &= \frac{1}{\varepsilon_{11}} D_x - \frac{\varepsilon_{12}}{\varepsilon_{11}} E_y - \frac{\varepsilon_{13}}{\varepsilon_{11}} E_z, \\ H_x &= \frac{1}{\mu_{11}} B_x - \frac{\mu_{12}}{\mu_{11}} H_y - \frac{\mu_{13}}{\mu_{11}} H_z \end{aligned} \quad (4.1.44)$$

and substitute into Maxwell's equations (4.1.28). As a result, we obtain:

$$\left\{ \begin{aligned} \frac{\partial E_z}{\partial y} - \frac{\partial E_y}{\partial z} &= ik_0 B_x, \\ \frac{\partial E_x}{\partial z} - \frac{\partial E_z}{\partial x} &= ik_0 \left( \frac{\mu_{2,1}}{\mu_{1,1}} B_x + \left( \mu_{2,2} - \mu_{2,1} \frac{\mu_{1,2}}{\mu_{1,1}} \right) H_y + \left( \mu_{2,3} - \mu_{2,1} \frac{\mu_{1,3}}{\mu_{1,1}} \right) H_z \right), \\ \frac{\partial E_y}{\partial x} - \frac{\partial E_x}{\partial y} &= ik_0 \left( \frac{\mu_{3,1}}{\mu_{1,1}} B_x + \left( \mu_{3,2} - \mu_{3,1} \frac{\mu_{1,2}}{\mu_{1,1}} \right) H_y + \left( \mu_{3,3} - \mu_{3,1} \frac{\mu_{1,3}}{\mu_{1,1}} \right) H_z \right), \\ \frac{\partial H_z}{\partial y} - \frac{\partial H_y}{\partial z} &= -ik_0 D_x, \\ \frac{\partial H_x}{\partial z} - \frac{\partial H_z}{\partial x} &= -ik_0 \left( \frac{\varepsilon_{2,1}}{\varepsilon_{1,1}} D_x + \left( \varepsilon_{2,2} - \varepsilon_{2,1} \frac{\varepsilon_{1,2}}{\varepsilon_{1,1}} \right) E_y + \left( \varepsilon_{2,3} - \varepsilon_{2,1} \frac{\varepsilon_{1,3}}{\varepsilon_{1,1}} \right) E_z \right), \\ \frac{\partial H_y}{\partial x} - \frac{\partial H_x}{\partial y} &= -ik_0 \left( \frac{\varepsilon_{3,1}}{\varepsilon_{1,1}} D_x + \left( \varepsilon_{3,2} - \varepsilon_{3,1} \frac{\varepsilon_{1,2}}{\varepsilon_{1,1}} \right) E_y + \left( \varepsilon_{3,3} - \varepsilon_{3,1} \frac{\varepsilon_{1,3}}{\varepsilon_{1,1}} \right) E_z \right). \end{aligned} \right. \quad (4.1.45)$$

Equations (1.4.45) do not contain products of functions showing discontinuities at the same time. Accordingly, in the transition to the space-frequency domain we can use the direct Laurent rule (4.1.31), (4.1.32). According to (4.1.44), the vectors of the Fourier coefficients of the functions  $D_x$ ,  $B_x$  have the form

$$\begin{aligned}
[D_x] &= \left[ \frac{1}{\varepsilon_{11}} \right]^{-1} \left( [E_x] + \left[ \frac{\varepsilon_{12}}{\varepsilon_{11}} \right] [E_y] + \left[ \frac{\varepsilon_{13}}{\varepsilon_{11}} \right] [E_z] \right), \\
[B_x] &= \left[ \frac{1}{\mu_{11}} \right]^{-1} \left( [H_x] + \left[ \frac{\mu_{12}}{\mu_{11}} \right] [H_y] + \left[ \frac{\mu_{13}}{\mu_{11}} \right] [H_z] \right).
\end{aligned} \tag{4.1.46}$$

Performing in (1.4.45) the transition to the space–frequency domain and performing transformations, we obtain a system of differential equations (1.4.36)–(4.1.38), where the matrices  $\mathbf{M}_{ij}$  and  $\mathbf{E}_{ij}$  have the form:

$$\begin{aligned}
\mathbf{M}_{1,1} &= \left[ \frac{1}{\mu_{11}} \right]^{-1}, \quad \mathbf{M}_{1,2} = \left[ \frac{1}{\mu_{11}} \right]^{-1} \left[ \frac{\mu_{12}}{\mu_{11}} \right], \quad \mathbf{M}_{1,3} = \left[ \frac{1}{\mu_{11}} \right]^{-1} \left[ \frac{\mu_{13}}{\mu_{11}} \right], \\
\mathbf{M}_{2,1} &= \left[ \frac{\mu_{21}}{\mu_{11}} \right] \left[ \frac{1}{\mu_{11}} \right]^{-1}, \quad \mathbf{M}_{2,2} = \left[ \mu_{22} - \frac{\mu_{12}\mu_{21}}{\mu_{11}} \right] + \left[ \frac{\mu_{21}}{\mu_{11}} \right] \left[ \frac{1}{\mu_{11}} \right]^{-1} \left[ \frac{\mu_{12}}{\mu_{11}} \right], \\
\mathbf{M}_{2,3} &= \left[ \mu_{23} - \frac{\mu_{13}\mu_{21}}{\mu_{11}} \right] + \left[ \frac{\mu_{21}}{\mu_{11}} \right] \left[ \frac{1}{\mu_{11}} \right]^{-1} \left[ \frac{\mu_{13}}{\mu_{11}} \right], \\
\mathbf{M}_{3,1} &= \left[ \frac{\mu_{31}}{\mu_{11}} \right] \left[ \frac{1}{\mu_{11}} \right]^{-1}, \quad \mathbf{M}_{3,2} = \left[ \mu_{32} - \frac{\mu_{31}\mu_{12}}{\mu_{11}} \right] + \left[ \frac{\mu_{31}}{\mu_{11}} \right] \left[ \frac{1}{\mu_{11}} \right]^{-1} \left[ \frac{\mu_{12}}{\mu_{11}} \right], \\
\mathbf{M}_{3,3} &= \left[ \mu_{33} - \frac{\mu_{31}\mu_{13}}{\mu_{11}} \right] + \left[ \frac{\mu_{31}}{\mu_{11}} \right] \left[ \frac{1}{\mu_{11}} \right]^{-1} \left[ \frac{\mu_{13}}{\mu_{11}} \right], \\
\mathbf{E}_{1,1} &= \left[ \frac{1}{\varepsilon_{11}} \right]^{-1}, \quad \mathbf{E}_{1,2} = \left[ \frac{1}{\varepsilon_{11}} \right]^{-1} \left[ \frac{\varepsilon_{12}}{\varepsilon_{11}} \right], \quad \mathbf{E}_{1,3} = \left[ \frac{1}{\varepsilon_{11}} \right]^{-1} \left[ \frac{\varepsilon_{13}}{\varepsilon_{11}} \right], \\
\mathbf{E}_{2,1} &= \left[ \frac{\varepsilon_{21}}{\varepsilon_{11}} \right] \left[ \frac{1}{\varepsilon_{11}} \right]^{-1}, \quad \mathbf{E}_{2,2} = \left[ \varepsilon_{22} - \frac{\varepsilon_{12}\varepsilon_{21}}{\varepsilon_{11}} \right] + \left[ \frac{\varepsilon_{21}}{\varepsilon_{11}} \right] \left[ \frac{1}{\varepsilon_{11}} \right]^{-1} \left[ \frac{\varepsilon_{12}}{\varepsilon_{11}} \right], \\
\mathbf{E}_{2,3} &= \left[ \varepsilon_{23} - \frac{\varepsilon_{13}\varepsilon_{21}}{\varepsilon_{11}} \right] + \left[ \frac{\varepsilon_{21}}{\varepsilon_{11}} \right] \left[ \frac{1}{\varepsilon_{11}} \right]^{-1} \left[ \frac{\varepsilon_{13}}{\varepsilon_{11}} \right], \\
\mathbf{E}_{3,1} &= \left[ \frac{\varepsilon_{31}}{\varepsilon_{11}} \right] \left[ \frac{1}{\varepsilon_{11}} \right]^{-1}, \quad \mathbf{E}_{3,2} = \left[ \varepsilon_{32} - \frac{\varepsilon_{31}\varepsilon_{12}}{\varepsilon_{11}} \right] + \left[ \frac{\varepsilon_{31}}{\varepsilon_{11}} \right] \left[ \frac{1}{\varepsilon_{11}} \right]^{-1} \left[ \frac{\varepsilon_{12}}{\varepsilon_{11}} \right], \\
\mathbf{E}_{3,3} &= \left[ \varepsilon_{33} - \frac{\varepsilon_{31}\varepsilon_{13}}{\varepsilon_{11}} \right] + \left[ \frac{\varepsilon_{31}}{\varepsilon_{11}} \right] \left[ \frac{1}{\varepsilon_{11}} \right]^{-1} \left[ \frac{\varepsilon_{13}}{\varepsilon_{11}} \right].
\end{aligned} \tag{4.1.47}$$

The system of the differential equations (1.4.36) with the matrices  $\mathbf{M}_{ij}$ ,  $\mathbf{E}_{ij}$  in the form of (1.4.47) is called a system, obtained using the correct rules of the Fourier expansions for the products of functions.

### Form of the matrix of the system at different dielectric permittivity tensors

We consider some special types of dielectric tensors and the corresponding matrices of the system of differential equations (4.1.36)–(4.1.38). The systems of differential equations are given for the case of correct rules for Fourier expansions.

Consider the case of an isotropic material. For an isotropic material  $\mu = 1$ , and  $\varepsilon$  are scalars. In this case the  $\mathbf{E}_{ij}$ ,  $\mathbf{M}_{ij}$  matrices take the following form:

$$\begin{aligned} \mathbf{E}_{1,1} = \mathbf{E}^* &= \left[ \frac{1}{\varepsilon} \right]^{-1}, \quad \mathbf{E}_{2,2} = \mathbf{E}_{3,3} = \mathbf{E} = [\varepsilon], \\ \mathbf{E}_{1,2} = \mathbf{E}_{1,3} = \mathbf{E}_{2,1} = \mathbf{E}_{2,3} = \mathbf{E}_{3,1} = \mathbf{E}_{3,2} &= \mathbf{0}, \\ \mathbf{M}_{1,1} = \mathbf{M}_{2,2} = \mathbf{M}_{3,3} &= \mathbf{I}, \\ \mathbf{M}_{1,2} = \mathbf{M}_{1,3} = \mathbf{M}_{2,1} = \mathbf{M}_{2,3} = \mathbf{M}_{3,1} = \mathbf{M}_{3,2} &= \mathbf{0}, \end{aligned} \quad (4.1.48)$$

where  $\mathbf{I}$  is the identity matrix of dimension  $(2N+1) \times (2N+1)$ . Substituting (4.1.48) into (4.1.37)–(4.1.38), we obtain a matrix of the system of differential equations in the form of:

$$\mathbf{A} = - \begin{bmatrix} \mathbf{0} & \mathbf{0} & \mathbf{K}_y \mathbf{E}^{-1} \mathbf{K}_x & \mathbf{I} - \mathbf{K}_y \mathbf{E}^{-1} \mathbf{K}_y \\ \mathbf{0} & \mathbf{0} & \mathbf{K}_x \mathbf{E}^{-1} \mathbf{K}_x - \mathbf{I} & -\mathbf{K}_x \mathbf{E}^{-1} \mathbf{K}_y \\ \mathbf{K}_y \mathbf{K}_x & \mathbf{E}^* - \mathbf{K}_y^2 & \mathbf{0} & \mathbf{0} \\ \mathbf{K}_x^2 - \mathbf{E} & -\mathbf{K}_x \mathbf{K}_y & \mathbf{0} & \mathbf{0} \end{bmatrix}. \quad (4.1.49)$$

Consider the case of plane incidence, where  $k_y = 0$  ( $\phi = 0$ ) as in (4.1.24) and the vector of direction of the incident wave vector lies in the plane  $XOZ$ . In this case  $\mathbf{K}_y = \mathbf{0}$  in (4.1.49) and the system of differential equations (4.1.36) splits into two independent systems

$$\begin{aligned} \frac{d}{dz'} \begin{bmatrix} \mathbf{U}_y \\ \mathbf{S}_x \end{bmatrix} &= \mathbf{A}^{TM} \begin{bmatrix} \mathbf{U}_y \\ \mathbf{S}_x \end{bmatrix}, \quad \mathbf{A}^{TM} = - \begin{bmatrix} \mathbf{0} & \mathbf{E}^* \\ \mathbf{K}_x \mathbf{E}^{-1} \mathbf{K}_x - \mathbf{I} & \mathbf{0} \end{bmatrix}, \\ \frac{d}{dz'} \begin{bmatrix} \mathbf{S}_y \\ \mathbf{U}_x \end{bmatrix} &= \mathbf{A}^{TE} \begin{bmatrix} \mathbf{S}_y \\ \mathbf{U}_x \end{bmatrix}, \quad \mathbf{A}^{TE} = - \begin{bmatrix} \mathbf{0} & \mathbf{I} \\ \mathbf{K}_x^2 - \mathbf{E} & \mathbf{0} \end{bmatrix}. \end{aligned} \quad (4.1.50)$$

In the case of plane incidence this result allows to reduce the solution of the diffraction problem to two independent problems of diffraction of waves with TM- and TE-polarization.

In section 4.3 we study structures containing layers of a magnetized material. For the magnetized materials the permittivity is given by the tensor [18, 19]:

$$\tilde{\boldsymbol{\varepsilon}} = \begin{bmatrix} \varepsilon & ig \cos \theta_M & -ig \sin \theta_M \sin \phi_M \\ -ig \cos \theta_M & \varepsilon & ig \sin \theta_M \cos \phi_M \\ ig \sin \theta_M \sin \phi_M & -ig \sin \theta_M \cos \phi_M & \varepsilon \end{bmatrix} \quad (4.1.51)$$

where  $\varepsilon$  is the main dielectric constant of the medium,  $g$  is the modulus of the gyration vector of the medium, proportional to the magnetization [18, 19],  $\theta_M$  and  $\phi_M$  are the spherical coordinates describing the direction of the magnetization vector. In the optical range  $\mu = 1$ .

We consider three basic cases, corresponding to the direction of the magnetization vector in three coordinate axes.

At vertical magnetization (magnetization vector perpendicular to the plane of the layers of the structure)  $\theta_M = 0$  and tensor (1.4.51) takes the form:

$$\vec{\varepsilon} = \begin{bmatrix} \varepsilon & ig & 0 \\ -ig & \varepsilon & 0 \\ 0 & 0 & \varepsilon \end{bmatrix}. \quad (4.1.52)$$

In this case,

$$\mathbf{A} = - \begin{bmatrix} \mathbf{0} & \mathbf{0} & \mathbf{K}_y \mathbf{E}^{-1} \mathbf{K}_x & \mathbf{I} - \mathbf{K}_y \mathbf{E}^{-1} \mathbf{K}_y \\ \mathbf{0} & \mathbf{0} & \mathbf{K}_x \mathbf{E}^{-1} \mathbf{K}_x - \mathbf{I} & -\mathbf{K}_x \mathbf{E}^{-1} \mathbf{K}_y \\ i \mathbf{E}^* \mathbf{H} + \mathbf{K}_y \mathbf{K}_x & \mathbf{E}^* - \mathbf{K}_y^2 & \mathbf{0} & \mathbf{0} \\ \mathbf{K}_x^2 - \mathbf{E}_2 & i \mathbf{H} \mathbf{E}^* - \mathbf{K}_x \mathbf{K}_y & \mathbf{0} & \mathbf{0} \end{bmatrix}, \quad (4.1.53)$$

where  $\mathbf{E}^* = \left[ \left[ \frac{1}{\varepsilon} \right] \right]^{-1}$ ,  $\mathbf{E} = \llbracket \varepsilon \rrbracket$ ,  $\mathbf{H} = \left[ \left[ \frac{g}{\varepsilon} \right] \right]$ ,  $\mathbf{E}_2 = \left[ \left[ \varepsilon - \frac{g^2}{\varepsilon} \right] \right] + \mathbf{H} \mathbf{E}^* \mathbf{H}$ .

For horizontal magnetization (magnetization vector is parallel to the layer plane and directed along the axis Ox)  $\theta_M = \frac{\pi}{2}$ ,  $M = 0$ , and tensor (1.4.51) takes the form

$$\vec{\varepsilon} = \begin{bmatrix} \varepsilon & 0 & 0 \\ 0 & \varepsilon & ig \\ 0 & -ig & \varepsilon \end{bmatrix}. \quad (4.1.54)$$

In the case of (4.1.54), the matrix of the system takes the form

$$\mathbf{A} = - \begin{bmatrix} \mathbf{K}_y \mathbf{E}^{-1} \mathbf{G} & \mathbf{0} & \mathbf{K}_y \mathbf{E}^{-1} \mathbf{K}_x & \mathbf{I} - \mathbf{K}_y \mathbf{E}^{-1} \mathbf{K}_y \\ \mathbf{K}_x \mathbf{E}^{-1} \mathbf{G} & \mathbf{0} & \mathbf{K}_x \mathbf{E}^{-1} \mathbf{K}_x - \mathbf{I} & -\mathbf{K}_x \mathbf{E}^{-1} \mathbf{K}_y \\ \mathbf{K}_y \mathbf{K}_x & \mathbf{E}^* - \mathbf{K}_y^2 & \mathbf{0} & \mathbf{0} \\ \mathbf{G} \mathbf{E}^{-1} \mathbf{G} + \mathbf{K}_x^2 - \mathbf{E} & -\mathbf{K}_x \mathbf{K}_y & \mathbf{G} \mathbf{E}^{-1} \mathbf{K}_x & -\mathbf{G} \mathbf{E}^{-1} \mathbf{K}_y \end{bmatrix}, \quad (4.1.55)$$

where  $\mathbf{G} = \llbracket [g] \rrbracket$ .

At the direction of the magnetization vector along the axis Oy  $\theta_M = \varphi_M = \frac{\pi}{2}$ . In this case from (1.4.51) we get:

$$\bar{\mathbf{e}} = \begin{bmatrix} \varepsilon & 0 & ig \\ 0 & \varepsilon & 0 \\ -ig & 0 & \varepsilon \end{bmatrix}. \quad (4.1.56)$$

For the tensor (4.1.56), the matrix of the system takes the form

$$\mathbf{A} = - \begin{bmatrix} \mathbf{0} & \mathbf{K}_y \mathbf{E}_2^{-1} \mathbf{H} \mathbf{E}^* & \mathbf{K}_y \mathbf{E}_2^{-1} \mathbf{K}_x & \mathbf{I} - \mathbf{K}_y \mathbf{E}_2^{-1} \mathbf{K}_y \\ \mathbf{0} & \mathbf{K}_x \mathbf{E}_2^{-1} \mathbf{H} \mathbf{E}^* & \mathbf{K}_x \mathbf{E}_2^{-1} \mathbf{K}_x - \mathbf{I} & -\mathbf{K}_x \mathbf{E}_2^{-1} \mathbf{K}_y \\ \mathbf{K}_y \mathbf{K}_x & \mathbf{E}^* - \mathbf{K}_y^2 - \mathbf{E}^* \mathbf{H} \mathbf{E}_2^{-1} \mathbf{H} \mathbf{E}^* & -\mathbf{E}^* \mathbf{H} \mathbf{E}_2^{-1} \mathbf{K}_x & \mathbf{E}^* \mathbf{H} \mathbf{E}_2^{-1} \mathbf{K}_y \\ \mathbf{K}_x^2 - \mathbf{E} & -\mathbf{K}_x \mathbf{K}_y & \mathbf{0} & \mathbf{0} \end{bmatrix}. \quad (4.1.57)$$

where  $\mathbf{E}_2 = \left[ \left[ \varepsilon - \frac{g^2}{\varepsilon} \right] \right] + \mathbf{H} \mathbf{E}^* \mathbf{H}$ .

#### 4.1.2.4. Presentation of the field inside the layer

To directly view the field in the layer, we examine the natural decomposition of the matrix:

$$\mathbf{A} = \mathbf{W} \mathbf{\Lambda} \mathbf{W}^{-1}, \quad (4.1.58)$$

where  $\mathbf{\Lambda} = \text{diag } \lambda_i$  is the diagonal matrix of the eigenvalues of the matrix  $\mathbf{A}$ , and  $\mathbf{W}$  is the  $i$  matrix of eigenvectors. Then the solution of systems of differential equations (1.4.36) can be written as:

$$\begin{bmatrix} \mathbf{S}_y \\ \mathbf{S}_x \\ \mathbf{U}_y \\ \mathbf{U}_x \end{bmatrix} = \mathbf{W} \exp(\mathbf{\Lambda} z') \mathbf{C}' = \mathbf{W} \exp(\mathbf{\Lambda} k_0 z) \mathbf{C}' = \sum_i c'_i w_i \exp(\lambda_i k_0 z). \quad (4.1.59)$$

We split the last sum into two, depending on the sign of the real part  $\lambda_i$  and write the expression in matrix notation:

$$\begin{aligned} \begin{bmatrix} \mathbf{S}_y \\ \mathbf{S}_x \\ \mathbf{U}_y \\ \mathbf{U}_x \end{bmatrix} &= \sum_i c'_i w_i \exp(\lambda_i k_0 z) = \\ &= \sum_{i: \text{Re} \lambda_i < 0} c_i w_i \exp(\lambda_i k_0 (z - d_l)) + \sum_{i: \text{Re} \lambda_i > 0} c_i w_i \exp(\lambda_i k_0 (z - d_{l-1})) = \\ &= \mathbf{W}^{(-)} \exp(\mathbf{\Lambda}^{(-)} k_0 (z - d_l)) \mathbf{C}^{(-)} + \mathbf{W}^{(+)} \exp(\mathbf{\Lambda}^{(+)} k_0 (z - d_{l-1})) \mathbf{C}^{(+)}, \end{aligned} \quad (4.1.60)$$

where  $\Lambda^{(+)}$  and  $\Lambda^{(-)}$  are the diagonal matrices of eigenvalues whose real parts are positive and negative, respectively,  $\mathbf{W}^{(+)}$  and  $\mathbf{W}^{(-)}$  are the corresponding matrices of eigenvectors,  $\mathbf{C}^{(-)}$ ,  $\mathbf{C}^{(+)}$  are the vectors of arbitrary constants. The representation (1.4.60) is focused on computer calculation. The exponents in (4.1.60) always have a negative real part. This ensures that no overflow occurs.

In some cases, the procedure to calculate the eigenvectors and eigenvalues can be greatly speeded up taking into account the special form of the matrix  $\mathbf{A}$  [4]. In particular, the matrix  $A$  in (4.1.49), (4.1.50), (4.1.53) has the following block structure

$$\mathbf{A} = \begin{bmatrix} \mathbf{0} & \mathbf{A}_{12} \\ \mathbf{A}_{21} & \mathbf{0} \end{bmatrix}. \quad (4.1.61)$$

We write for  $\mathbf{A}$  the matrices of eigenvectors and eigenvalues as

$$\mathbf{W} = \begin{bmatrix} \mathbf{W}_{11} & \mathbf{W}_{12} \\ \mathbf{W}_{21} & \mathbf{W}_{22} \end{bmatrix}, \quad \Lambda = \begin{bmatrix} \Lambda_{11} & \mathbf{0} \\ \mathbf{0} & \Lambda_{22} \end{bmatrix}. \quad (4.1.62)$$

Since  $\mathbf{A} = \mathbf{W} \Lambda \mathbf{W}^{-1}$ , then

$$\begin{aligned} \begin{bmatrix} \mathbf{0} & \mathbf{A}_{12} \\ \mathbf{A}_{21} & \mathbf{0} \end{bmatrix} \cdot \begin{bmatrix} \mathbf{W}_{11} & \mathbf{W}_{12} \\ \mathbf{W}_{21} & \mathbf{W}_{22} \end{bmatrix} &= \begin{bmatrix} \mathbf{W}_{11} & \mathbf{W}_{12} \\ \mathbf{W}_{21} & \mathbf{W}_{22} \end{bmatrix} \cdot \begin{bmatrix} \Lambda_{11} & \mathbf{0} \\ \mathbf{0} & \Lambda_{22} \end{bmatrix}, \\ \begin{bmatrix} \mathbf{A}_{12} \mathbf{W}_{21} & \mathbf{A}_{12} \mathbf{W}_{22} \\ \mathbf{A}_{21} \mathbf{W}_{11} & \mathbf{A}_{21} \mathbf{W}_{12} \end{bmatrix} &= \begin{bmatrix} \mathbf{W}_{11} \Lambda_{11} & \mathbf{W}_{12} \Lambda_{22} \\ \mathbf{W}_{21} \Lambda_{11} & \mathbf{W}_{22} \Lambda_{22} \end{bmatrix} \end{aligned}$$

and we have

$$\begin{aligned} \mathbf{A}_{12} \mathbf{A}_{21} \mathbf{W}_{11} &= \mathbf{A}_{12} \mathbf{W}_{21} \Lambda_{11} = \mathbf{W}_{11} \Lambda_{11} \Lambda_{11}, \\ \mathbf{A}_{12} \mathbf{A}_{21} \mathbf{W}_{12} &= \mathbf{A}_{12} \mathbf{W}_{22} \Lambda_{22} = \mathbf{W}_{12} \Lambda_{22} \Lambda_{22}. \end{aligned} \quad (4.1.63)$$

We introduce the matrix  $\mathbf{B} = \mathbf{A}_{12} \mathbf{A}_{21}$  and represent (4.1.63) as

$$\mathbf{B} \cdot \mathbf{W}_{11} = \mathbf{W}_{11} \Lambda_{11}^2, \quad \mathbf{B} \cdot \mathbf{W}_{12} = \mathbf{W}_{12} \Lambda_{22}^2. \quad (4.1.64)$$

According to (4.1.64)  $\mathbf{W}_{11}$ ,  $\Lambda_{11}^2$ ,  $\mathbf{W}_{12}$ ,  $\Lambda_{22}^2$  are the matrixes of eigenvectors and diagonal matrices of eigenvalues of the same matrix  $\mathbf{B}$ . So

$$\mathbf{W}_{11} = \mathbf{W}_{12}, \quad \Lambda_{22} = -\Lambda_{11} \text{ and } \mathbf{W}_{21} = \mathbf{A}_{21} \mathbf{W}_{11} \Lambda_{11}^{-1}, \quad \mathbf{W}_{22} = -\mathbf{W}_{21}. \quad (4.1.65)$$

The relations (1.4.65) determine the eigenvalues and eigenvectors of the matrix  $\mathbf{A}$  through the eigenvalues and eigenvectors of the matrix  $\mathbf{B}$  twice smaller in the form of:

$$\mathbf{W} = \begin{bmatrix} \mathbf{W}_{11} & \mathbf{W}_{11} \\ \mathbf{A}_{21} \mathbf{W}_{11} \Lambda_{11}^{-1} & -\mathbf{A}_{21} \mathbf{W}_{11} \Lambda_{11}^{-1} \end{bmatrix}, \quad \Lambda = \begin{bmatrix} \sqrt{\Lambda_{11}} & 0 \\ 0 & -\sqrt{\Lambda_{11}} \end{bmatrix}. \quad (4.1.66)$$

In [4] it is noted that halving the dimension of the eigenvalue problem to eigenvalues is equivalent to reducing system (36) from  $4(2N+1)$  first order differential equations to a system  $2(2N+1)$  of second order differential equations.

#### 4.1.2.5. 'Stitching' of the electromagnetic field on the layer boundaries

The general representation of the field in the layer was described above. To obtain a solution which satisfies the Maxwell equations, it is necessary to equate the tangential field components at the layer boundaries. Equating the tangential field components is equivalent to equating functions (4.1.60) with the meaning of the Fourier coefficients for each fixed  $z$ . We write the preliminary solutions (4.1.60) on the upper and lower boundaries of all layers. For convenience, we assume that the matrix of eigenvectors  $\mathbf{W}$  is given by:

$$\mathbf{W} = \begin{bmatrix} \mathbf{W}^{(-)} & \mathbf{W}^{(+)} \end{bmatrix}. \quad (4.1.67)$$

In addition, we introduce the vector of unknown constants  $\mathbf{C}$  as follows:

$$\mathbf{C} = \begin{bmatrix} \mathbf{C}^{(-)} \\ \mathbf{C}^{(+)} \end{bmatrix}. \quad (4.1.68)$$

Given this notation the solution of (4.1.60) on the upper and lower boundaries of the layer has the form

$$\begin{bmatrix} \mathbf{S}_y(d_{l-1}) \\ \mathbf{S}_x(d_{l-1}) \\ \mathbf{U}_y(d_{l-1}) \\ \mathbf{U}_x(d_{l-1}) \end{bmatrix} = \mathbf{W}^{(-)} \mathbf{x}^{(-)} \mathbf{C}^{(-)} + \mathbf{W}^{(+)} \mathbf{C}^{(+)} = \mathbf{W} \begin{bmatrix} \mathbf{x}^{(-)} & \mathbf{0} \\ \mathbf{0} & \mathbf{I} \end{bmatrix} \mathbf{C} = \mathbf{N}\mathbf{C}, \quad (4.1.69)$$

$$\begin{bmatrix} \mathbf{S}_y(d_l) \\ \mathbf{S}_x(d_l) \\ \mathbf{U}_y(d_l) \\ \mathbf{U}_x(d_l) \end{bmatrix} = \mathbf{W}^{(-)} \mathbf{C}^{(-)} + \mathbf{W}^{(+)} \mathbf{x}^{(+)} \mathbf{C}^{(+)} = \mathbf{W} \begin{bmatrix} \mathbf{I} & \mathbf{0} \\ \mathbf{0} & \mathbf{x}^{(+)} \end{bmatrix} \mathbf{C} = \mathbf{M}\mathbf{C}, \quad (4.1.70)$$

where

$$\mathbf{x}^{(+)} = \exp(\mathbf{\Lambda}^{(+)} k_0 (d_l - d_{l-1})), \quad \mathbf{x}^{(-)} = \exp(\mathbf{\Lambda}^{(-)} k_0 (d_{l-1} - d_l)). \quad (4.1.71)$$

Equating the tangential components at the interface between adjacent layers, we obtain the equation

$$\mathbf{M}_{i-1} \mathbf{C}_{i-1} = \mathbf{N}_i \mathbf{C}_i, \quad i = 2, \dots, L, \quad (4.1.72)$$

where the index  $i = 2$  corresponds to the condition at the lower boundary of the upper layer, the index  $i = L$  – at the upper boundary of the lower layer.

The relations (4.1.72) must be supplemented by the conditions of equality of the tangential components of the field above the structure (4.1.22) and at the upper boundary of the 1st layer, as well as of the field under the structure (1.4.23) and at the lower boundary of the  $L$ -th layer. Given the fact that in the layers of the field components are represented by segments of Fourier series of dimension  $2N+1$  in the representations in the fields above and below the grating (4.1.22)–(4.1.24) it is necessary to take  $2N + 1$  waves at  $-N \leq i \leq N$ .

By adding these relations for the upper and lower boundaries of the diffraction structure, we obtain the following system of linear equations:

$$\begin{cases} \mathbf{D} + \mathbf{P}\mathbf{R} = \mathbf{N}_1\mathbf{C}_1, \\ \mathbf{M}_{i-1}\mathbf{C}_{i-1} = \mathbf{N}_i\mathbf{C}_i, \quad i = 2, \dots, L, \\ \mathbf{M}_L\mathbf{C}_L = \mathbf{F}\mathbf{T}, \end{cases} \quad (4.1.73)$$

where  $\mathbf{R}$  and  $\mathbf{T}$  are the vectors of complex amplitudes of reflected and transmitted orders, respectively. These vectors have the form:

$$\mathbf{R} = \begin{bmatrix} \mathbf{R}_E \\ \mathbf{R}_H \end{bmatrix}, \quad \mathbf{T} = \begin{bmatrix} \mathbf{T}_E \\ \mathbf{T}_H \end{bmatrix}, \quad (4.1.74)$$

$\mathbf{R}_E$  and  $\mathbf{T}_E$  are the the vectors of complex amplitudes of  $E$ -waves,  $\mathbf{R}_H$  and  $\mathbf{T}_H$  are the vectors of complex amplitudes of  $H$ -waves.

The vector  $\mathbf{D}$  in (1.4.73) represents the incident wave and has the form:

$$\mathbf{D} = \begin{bmatrix} \cos \theta \sin \phi \cdot \boldsymbol{\delta}_i \\ \cos \theta \cos \phi \cdot \boldsymbol{\delta}_i \\ -in_1 \cos \phi \cdot \boldsymbol{\delta}_i \\ in_1 \sin \phi \cdot \boldsymbol{\delta}_i \end{bmatrix} \cos \psi + \begin{bmatrix} \cos \phi \cdot \boldsymbol{\delta}_i \\ -\sin \phi \cdot \boldsymbol{\delta}_i \\ in_1 \cos \theta \sin \phi \cdot \boldsymbol{\delta}_i \\ in_1 \cos \theta \cos \phi \cdot \boldsymbol{\delta}_i \end{bmatrix} \sin \psi, \quad (4.1.75)$$

where  $\boldsymbol{\delta}_i$  is a column vector, in which only one element in the middle is different from zero and unity. The column vector  $\boldsymbol{\delta}_i$  has the dimension  $2N + 1$ , vector  $\mathbf{D}$  – dimension  $4(2N+1)$ .

The matrixes  $\mathbf{P}$  and  $\mathbf{F}$  in (1.4.73) correspond to the reflected and transmitted orders, respectively, and have the form

$$\mathbf{P} = \begin{bmatrix} -n_1 \cos \Theta^{(1)} \sin \Phi & \cos \Phi \\ -n_1 \cos \Theta^{(1)} \cos \Phi & -\sin \Phi \\ -in_1^2 \cos \Phi & -in_1 \cos \Theta^{(1)} \sin \Phi \\ in_1^2 \sin \Phi & -in_1 \cos \Theta^{(1)} \cos \Phi \end{bmatrix}, \quad (4.1.76)$$

$$\mathbf{F} = \begin{bmatrix} -n_2 \cos \Theta^{(2)} \sin \Phi & \cos \Phi \\ -n_2 \cos \Theta^{(2)} \cos \Phi & -\sin \Phi \\ -in_2^2 \cos \Phi & -in_2 \cos \Theta^{(2)} \sin \Phi \\ in_2^2 \sin \Phi & -in_2 \cos \Theta^{(2)} \cos \Phi \end{bmatrix}, \quad (4.1.77)$$

where  $\Phi$ ,  $\Theta^{(1)}$ ,  $\Theta^{(2)}$  are the diagonal matrices of angles corresponding to diffraction orders. They satisfy the following relations:

$$\sin \Phi = \text{diag}_i \frac{k_y}{\sqrt{k_{x,i}^2 + k_y^2}}, \quad \cos \Phi = \text{diag}_i \frac{k_{x,i}}{\sqrt{k_{x,i}^2 + k_y^2}}, \quad (4.1.78)$$

$$\cos \Theta^{(1)} = \text{diag}_i \frac{-k_{z,I,i}}{k_0 n_1^2}, \quad \cos \Theta^{(2)} = \text{diag}_i \frac{k_{z,II,i}}{k_0 n_2^2}. \quad (4.1.79)$$

The expressions (1.4.75)–(4.1.77) follow directly from the general formulas (4.1.12), (4.1.13) for a plane wave taking into account the type of propagation constants of the orders (4.1.24).

According to (1.4.73), the solution of the diffraction problem is reduced to solving a system of linear equations. Sequential exclusion of the coefficients  $\mathbf{C}_i$  in (4.1.73) reduces the system (1.4.73) to a system of equations for the coefficients  $\mathbf{R}$  and  $\mathbf{T}$ . Indeed, from the last two equations in (4.1.73) we obtain

$$\mathbf{M}_{L-1} \mathbf{C}_{L-1} = \mathbf{N}_L \mathbf{M}_L^{-1} \mathbf{F} \mathbf{T}. \quad (4.1.80)$$

Substituting (1.4.80) into the equation with the index  $i = L - 1$  in (4.1.73), we obtain

$$\mathbf{M}_{L-2} \mathbf{C}_{L-2} = \mathbf{N}_{L-1} \mathbf{M}_{L-1}^{-1} \mathbf{N}_L \mathbf{M}_L^{-1} \mathbf{F} \mathbf{T}. \quad (4.1.81)$$

Continuing this process to the equation with the index  $i = 2$ , we have

$$\mathbf{M}_1 \mathbf{C}_1 = \prod_{i=2}^L \mathbf{N}_i \mathbf{M}_i^{-1} \mathbf{F} \mathbf{T}. \quad (4.1.82)$$

Finally, substituting (1.4.82) in the first equation of (1.4.73), we obtain the desired system of linear equations for the coefficients  $\mathbf{R}$  and  $\mathbf{T}$  in the form of:

$$\mathbf{D} + \mathbf{P} \mathbf{R} = \left( \prod_{i=1}^L \mathbf{N}_i \mathbf{M}_i^{-1} \right) \mathbf{F} \mathbf{T}. \quad (4.1.83)$$

#### 4.1.2.6. Numerical and steady implementation of the method

Recording system in the form (4.1.83) can lead to a numerical instability of the problem [3]. Problems are associated with the calculation of the matrix

$$\mathbf{M}_i^{-1} = \left( \mathbf{W}_i \begin{bmatrix} \mathbf{I} & \mathbf{0} \\ \mathbf{0} & \mathbf{x}_i^{(+)} \end{bmatrix} \right)^{-1} = \begin{bmatrix} \mathbf{I} & \mathbf{0} \\ \mathbf{0} & (\mathbf{x}_i^{(+)})^{-1} \end{bmatrix} \mathbf{W}_i^{-1} \quad (4.1.84)$$

in (1.4.83). The diagonal matrix

$$(\mathbf{x}^{(+)})^{-1} = \exp(-\mathbf{\Lambda}_i^{(+)} k_0 (d_i - d_{i-1})) \quad (4.1.85)$$

contains the exponents of the positive values that can lead to overflow [3]. Consider the variant of writing a system of linear equations, avoiding computing the matrices (4.1.85). We denote

$$\mathbf{F}_L = \mathbf{F}, \quad \mathbf{T}^{(L)} = \mathbf{T}. \quad (4.1.86)$$

Given this notation, equation (1.4.83) takes the form

$$\mathbf{D} + \mathbf{P}\mathbf{R} = \left( \prod_{i=1}^L \mathbf{N}_i \mathbf{M}_i^{-1} \right) \mathbf{F}_L \mathbf{T}^{(L)}. \quad (4.1.87)$$

Transform (1.4.87) to the equation

$$\mathbf{D} + \mathbf{P}\mathbf{R} = \left( \prod_{i=1}^{L-1} \mathbf{N}_i \mathbf{M}_i^{-1} \right) \mathbf{F}_{L-1} \mathbf{T}^{(L-1)}, \quad (4.1.88)$$

where

$$\mathbf{F}_{L-1} \mathbf{T}^{(L-1)} = \mathbf{N}_L \mathbf{M}_L^{-1} \mathbf{F}_L \mathbf{T}^{(L)}. \quad (4.1.89)$$

Equation (4.1.88) has the same form as (4.1.87), but contains one less factor. Substituting into (4.1.89) the concrete form of matrices  $\mathbf{N}_L$  and  $\mathbf{M}_L^{-1}$ , we get

$$\mathbf{F}_{L-1} \mathbf{T}^{(L-1)} = \mathbf{W}_L \begin{bmatrix} \mathbf{x}_L^{(-)} & \mathbf{0} \\ \mathbf{0} & \mathbf{I} \end{bmatrix} \begin{bmatrix} \mathbf{I} & \mathbf{0} \\ \mathbf{0} & \mathbf{x}_L^{(+)} \end{bmatrix}^{-1} \mathbf{W}_L^{-1} \mathbf{F}_L \mathbf{T}^{(L)}. \quad (4.1.90)$$

We introduce the notation

$$\mathbf{A}_L = \begin{bmatrix} \mathbf{A}_L^{(-)} \\ \mathbf{A}_L^{(+)} \end{bmatrix} = \mathbf{W}_L^{-1} \mathbf{F}_L \quad (4.1.91)$$

and rewrite (4.1.90) to the form

$$\mathbf{F}_{L-1} \mathbf{T}^{(L-1)} = \mathbf{W}_L \begin{bmatrix} \mathbf{x}_L^{(-)} & \mathbf{0} \\ \mathbf{0} & \mathbf{I} \end{bmatrix} \begin{bmatrix} \mathbf{I} & \mathbf{0} \\ \mathbf{0} & \mathbf{x}_L^{(+)} \end{bmatrix}^{-1} \mathbf{A}_L \mathbf{T}^{(L)} = \mathbf{W}_L \begin{bmatrix} \mathbf{x}_L^{(-)} \mathbf{A}_L^{(-)} \\ (\mathbf{x}_L^{(+)})^{-1} \mathbf{A}_L^{(+)} \end{bmatrix} \mathbf{T}^{(L)}. \quad (4.1.92)$$

In order to avoid possible overflows in the calculation of the matrix  $(\mathbf{x}_L^{(+)})^{-1}$ , we draw the following substitution [3]

$$\mathbf{T}^{(L)} = \left( \mathbf{A}_L^{(+)} \right)^{-1} \mathbf{X}_L^{(+)} \mathbf{T}^{(L-1)}. \quad (4.1.93)$$

As a result, we obtain

$$\mathbf{F}_{L-1} \mathbf{T}^{(L-1)} = \mathbf{W}_L \begin{bmatrix} \mathbf{x}_L^{(-)} \mathbf{A}_L^{(-)} \left( \mathbf{A}_L^{(+)} \right)^{-1} \mathbf{x}_L^{(+)} \\ \mathbf{I} \end{bmatrix} \mathbf{T}^{(L-1)}. \quad (4.1.94)$$

Thus, the original system (4.1.87) is reduced to the system (1.4.88) of the same species, but containing at least one factor less. The transition to the system (1.4.88) is numerically stable. Numerical stability is achieved by replacing the variables (4.1.93).

By repeating these steps and successively reducing the number of factors in (4.1.88), we obtain the system

$$\mathbf{D} + \mathbf{P}\mathbf{R} = \mathbf{F}_0 \mathbf{T}^{(0)}. \quad (4.1.95)$$

The matrix  $\mathbf{F}^{(0)}$  in (1.4.95) can be calculated by successive application of recurrence relations

$$\mathbf{F}_{i-1} = \mathbf{W}_i \begin{bmatrix} \mathbf{x}_i^{(-)} \mathbf{A}_i^{(-)} \left( \mathbf{A}_i^{(+)} \right)^{-1} \mathbf{x}_i^{(+)} \\ \mathbf{I} \end{bmatrix}, \quad \begin{bmatrix} \mathbf{A}_i^{(-)} \\ \mathbf{A}_i^{(+)} \end{bmatrix} = \mathbf{W}_i^{-1} \mathbf{F}_i \quad (4.1.96)$$

with a decrease of the index  $i$  from  $L$  to 1. The solution of systems of linear equations determines the complex amplitudes of the reflected orders  $\mathbf{R}$  and vector  $\mathbf{T}^{(0)}$ . The amplitudes of the ??? orders  $\mathbf{T} = \mathbf{T}^{(L)}$  are determined through the consistent application of the formula (4.1.93):

$$\mathbf{T} = \mathbf{T}^{(L)} = \left( \mathbf{A}_L^{(+)} \right)^{-1} \mathbf{X}_L^{(+)} \cdot \left( \mathbf{A}_{L-1}^{(+)} \right)^{-1} \mathbf{X}_{L-1}^{(+)} \dots \left( \mathbf{A}_1^{(+)} \right)^{-1} \mathbf{X}_1^{(+)} \mathbf{T}^{(0)}. \quad (4.1.97)$$

Note that the expressions (1.4.93)–(1.4.97) can be obtained in the present form only in the case where the number of eigenvalues of the matrix  $\mathbf{A}$  with positive and negative signs of the real parts is equal. Otherwise  $\mathbf{A}_L^{(+)}$ , (1.4.91) will not be a square and then the inverse matrix  $(\mathbf{A}_L^{(+)})^{-1}$  cannot be used. In particular, the above condition for the eigenvalues is always satisfied for gratings of a homogeneous material and gratings of a magnetic material with a dielectric tensor in the form (1.4.52). It can be shown that this condition is also satisfied when the diffraction structure contains homogeneous magnetic layers with the dielectric tensor in the form of (4.1.54), (4.1.56).

#### 4.1.2.7. Characteristics of diffraction orders

In the analysis of the field outside the near zone of the grating the researcher is usually not interested in the complex amplitudes (4.1.74) and the intensity of the reflected and transmitted propagating diffraction orders. The propagating orders are determined by the actual values  $k_{z,i}$  in (4.1.24). The intensity of the diffraction orders is defined as the Umov–Pointing vector flux through the plane  $z = \text{const}$ , normalized to the flux of the incident wave [17]. Given the normalization (4.1.18) (4.1.19), the intensity of the orders can be found from the following expressions:

$$\mathbf{I}^R = \frac{\left| \text{Re}(\cos \Theta^{(1)}) \right|}{\cos \theta} \left( |n_1 \mathbf{R}_E|^2 + |\mathbf{R}_H|^2 \right), \quad (4.1.98)$$

$$\mathbf{I}^T = \frac{\left| n_2 \text{Re}(\cos \Theta^{(2)}) \right|}{n_1 \cos \theta} \left( |n_2 \mathbf{T}_E|^2 + |\mathbf{T}_H|^2 \right), \quad (4.1.99)$$

where the diagonal matrices  $\cos \Theta^{(1)}$ ,  $\cos \Theta^{(2)}$  are defined in (1.4.79), and the squaring of the vectors  $\mathbf{R}_E, \mathbf{R}_H, \mathbf{T}_E, \mathbf{T}_H$  is element-wise. For the decreasing diffraction orders  $\text{Re}(\cos \Theta^{(l)}) = 0$ ,  $l = 1, 2$ , respectively, their intensities are equal to zero.

In general, the propagating diffraction orders are plane waves with elliptical polarization. Indeed, each diffraction order corresponds to the superposition of the  $E$ - and  $H$ -waves. We denote by  $E_E, E_H$  the complex amplitudes of electric field vectors in the  $E$ - and  $H$ -waves. Note that the electric field vector of the  $E$ - and  $H$ -waves are perpendicular to each other and perpendicular to the direction of wave propagation. With the addition of perpendicular oscillations an elliptically polarized wave forms in a general case. The polarization ellipse is characterized by two parameters: the angle  $\varphi$  of the main axis of the polarization ellipse and the ellipticity parameter  $\chi$  [20]. The ellipticity parameter is the ratio of the lengths  $a, b$  of the axes of the polarization ellipse in the form  $\text{tg } \chi = a/b$ . The parameters are determined by the complex amplitudes  $E_E, E_H$  of the form [20]

$$\begin{aligned} \text{tg}(2\varphi) &= \frac{2 \text{Re}(E_E/E_H)}{1 - |E_E/E_H|^2}, \\ \sin(2\chi) &= \frac{2 \text{Im}(E_E/E_H)}{1 + |E_E/E_H|^2}. \end{aligned} \quad (4.1.100)$$

In conclusion, let us make some remarks on the choice of the parameter  $N$  that determines the length of the segments of the Fourier series approximating the components of the electric and magnetic fields in the zone of the grating. For a given  $N$  the number of calculated orders is equal to  $2N + 1$ , from  $-N$  to  $+N$ . The parameter  $N$  must be greater than the number of propagating orders. If the grating consists

of dielectrics only (all refractive indices are real numbers), and the parameter  $N$  satisfies the above condition, then the energy conservation law in the following form should be satisfied:

$$\sum I^R + \sum I^T = 1. \quad (4.1.101)$$

However, if the grating contains absorbing materials, the sum (4.1.101) should be less than unity. In general, the choice of  $N$  is made in the computational experiment from the conditions for stabilization of the values of the intensities of the orders.

### 4.1.3. Methods of Fourier modes in a three-dimensional case

Consider the described method for the case of three-dimensional periodic diffraction structures. The  $z$  axis is directed perpendicular to the plane of the grating. The functions of dielectric and magnetic permeabilities of the grating are assumed to be periodic with respect to variables  $x$ ,  $y$ , and with periods  $\Lambda_x$  and  $\Lambda_y$ , respectively. As in the planar case, we assume that the grating consists of  $L$  binary layers, and the dielectric permittivity and magnetic permeability in each layer does not depend on the variable  $z$ .

A method of solving the diffraction problem in three-dimensional case is similar to the considered two-dimensional case. Here are the main features of the three-dimensional problem.

In the diffraction of a plane wave in a three-dimensional diffraction grating formed by two-dimensional set of reflected and transmitted diffraction orders. In this case, the field above and below the structure is as follows:

$$\Phi^1(x, y, z) = \Phi^l(x, y, z) + \sum_n \sum_m \Phi_{n,m}^R(R_{n,m}) \exp(i(k_{x,n}x + k_{y,m}y + k_{z,l,n,m}z)), \quad (4.1.102)$$

$$\Phi^2(x, y, z) = \sum_n \sum_m \Phi_{n,m}^T(T_{n,m}) \exp(i(k_{x,n}x + k_{y,m}y - k_{z,l,n,m}(z - d_L))), \quad (4.1.103)$$

where  $\Phi^l(x, y, z)$  is the incident wave. We consider the incident wave given in the form (4.1.21). The propagation constants of the diffraction orders with the numbers  $(n, m)$  are described by the following expressions:

$$\begin{aligned} k_{x,n} &= k_0 \left( n_1 \sin \theta \cos \phi + n \frac{\lambda}{\Lambda_x} \right), \\ k_{y,m} &= k_0 \left( n_1 \sin \theta \sin \phi + m \frac{\lambda}{\Lambda_y} \right), \\ k_{z,l,n,m} &= \sqrt{(k_0 n_l)^2 - k_{x,n}^2 - k_{y,m}^2}, \end{aligned} \quad (4.1.104)$$

where the index  $l = 1$  is for the reflected orders and  $l = 2$  for the transmitted ones. The form of the propagation constants ensures fulfilling the two-dimensional

quasi-periodicity condition

$$\Phi^{1,2}(x + \Lambda_x, y + \Lambda_y, z) = \Phi^{1,2}(x, y, z) \exp(ik_{x,0}\Lambda_x + ik_{y,0}\Lambda_y). \quad (4.1.105)$$

According to (4.1.105), the amplitude of the field does not change with the shift to distances  $\Lambda_x, \Lambda_y$  multiplicable by time periods  $T_x, T_y$ . The waves with the real  $k_{z,l,n,m}$  are propagating, those with imaginary – damped.

The type of an electromagnetic field in each layer, as in the two-dimensional case, is described the basic Maxwell equations for monochromatic fields in the form (4.1.26)–(4.1.29). We represent the components of the electric and magnetic fields in the form of two-dimensional Fourier series with respect to the variables  $x, y$ :

$$\left\{ \begin{array}{l} E_x = \sum_n \sum_m S_{x,n,m}(z) \exp(i(k_{x,n}x + k_{y,m}y)), \\ E_y = \sum_n \sum_m S_{y,n,m}(z) \exp(i(k_{x,n}x + k_{y,m}y)), \\ E_z = \sum_n \sum_m S_{z,n,m}(z) \exp(i(k_{x,n}x + k_{y,m}y)), \\ H_x = -i \sum_n \sum_m U_{x,n,m}(z) \exp(i(k_{x,n}x + k_{y,m}y)), \\ H_y = -i \sum_n \sum_m U_{y,n,m}(z) \exp(i(k_{x,n}x + k_{y,m}y)), \\ H_z = -i \sum_n \sum_m U_{z,n,m}(z) \exp(i(k_{x,n}x + k_{y,m}y)). \end{array} \right. \quad (4.1.106)$$

The equations (4.1.106) are written taking into account the quasi-periodicity of the components of the fields in the variables  $x, y$ . We confine ourselves to the finite number of terms in the expansions (4.1.106), corresponding to  $-N_x \leq n \leq N_x, -N_y \leq m \leq N_y$ . Substituting (4.1.106) into the system (1.4.28) and equating the coefficients for the same Fourier harmonics, we obtain a system of differential equations in the form

$$\left\{ \begin{array}{l} ik_0 \mathbf{K}_y \mathbf{S}_z - \frac{d\mathbf{S}_y}{dz} = k_0 (\mathbf{M}_{1,1} \mathbf{U}_x + \mathbf{M}_{1,2} \mathbf{U}_y + \mathbf{M}_{1,3} \mathbf{U}_z), \\ \frac{d\mathbf{S}_x}{dz} - ik_0 \mathbf{K}_x \mathbf{S}_z = k_0 (\mathbf{M}_{2,1} \mathbf{U}_x + \mathbf{M}_{2,2} \mathbf{U}_y + \mathbf{M}_{2,3} \mathbf{U}_z), \\ ik_0 \mathbf{K}_x \mathbf{S}_y - ik_0 \mathbf{K}_y \mathbf{S}_x = k_0 (\mathbf{M}_{3,1} \mathbf{U}_x + \mathbf{M}_{3,2} \mathbf{U}_y + \mathbf{M}_{3,3} \mathbf{U}_z), \\ ik_0 \mathbf{K}_y \mathbf{U}_z - \frac{d\mathbf{U}_y}{dz} = k_0 (\mathbf{E}_{1,1} \mathbf{S}_x + \mathbf{E}_{1,2} \mathbf{S}_y + \mathbf{E}_{1,3} \mathbf{S}_z), \\ \frac{d\mathbf{U}_x}{dz} - ik_0 \mathbf{K}_x \mathbf{U}_z = k_0 (\mathbf{E}_{2,1} \mathbf{S}_x + \mathbf{E}_{2,2} \mathbf{S}_y + \mathbf{E}_{2,3} \mathbf{S}_z), \\ ik_0 \mathbf{K}_x \mathbf{U}_y - ik_0 \mathbf{K}_y \mathbf{U}_x = k_0 (\mathbf{E}_{3,1} \mathbf{S}_x + \mathbf{E}_{3,2} \mathbf{S}_y + \mathbf{E}_{3,3} \mathbf{S}_z). \end{array} \right. \quad (4.1.107)$$

The form of the resulting system is identical to that of the system (4.1.33) for the two-dimensional case. The difference lies in the particular representation of vectors and matrices in the system. The vectors  $\mathbf{S}_x, \mathbf{S}_y, \mathbf{S}_z, \mathbf{U}_x, \mathbf{U}_y, \mathbf{U}_z$  in (4.1.107) are progressive ??? of the matrices  $S_{x,j,k}, S_{y,j,k}, S_{z,j,k}, U_{x,j,k}, U_{y,j,k}, U_{z,j,k}, -N_x \leq j \leq N_x, -N_y \leq k \leq N_y$ . This means that the element of the vector  $\mathbf{S}_x$  with the number

$$l(i, j) = i(2N_y + 1) + j. \quad (4.1.108)$$

correspond to the value  $S_{x,i,j}$ . The vectors introduced in this way have the dimension  $(2N_x + 1)(2N_y + 1)$  equal to the total number of the calculated diffraction orders. For example, the vector  $\mathbf{S}_x$  has the form:

$$\mathbf{S}_x = \left[ S_{x,-N_x,-N_y}, S_{x,-N_x,1-N_y}, \dots, S_{x,-N_x,N_y}, S_{x,1-N_x,-N_y}, S_{x,1-N_x,1-N_y}, \dots, S_{x,N_x,N_y} \right]^T.$$

The matrices in  $\mathbf{K}_x, \mathbf{K}_y, \mathbf{E}_{i,j}, \mathbf{M}_{i,j}$  (4.1.107) have the dimension  $(2N_x+1)(2N_y+1) \times (2N_x+1)(2N_y+1)$ . The matrices  $\mathbf{K}_x$  and  $\mathbf{K}_y$  are determined by the following expressions:

$$\begin{aligned} K_{x,l(i,j),l(n,m)} &= k_{x,i} \delta_{i-n} \delta_{j-m} / k_0, \\ K_{y,l(i,j),l(n,m)} &= k_{y,j} \delta_{i-n} \delta_{j-m} / k_0, \end{aligned} \quad (4.1.109)$$

where  $-N_x \leq i, n \leq N_x, -N_y \leq j, m \leq N_y$ .

Consider the form of the matrices  $\mathbf{E}_{i,j}, \mathbf{M}_{i,j}$  obtained by using the normal Laurent rules for the expansion into Fourier series of the products of functions. The matrices  $\mathbf{E}_{i,j}, \mathbf{M}_{i,j}$  are composed of the Fourier coefficients of the tensors of dielectric permittivity and magnetic permeability, the structure of the matrices is the same and has the form

$$T_{l(i,j),l(n,m)} = e_{i-n,j-m}, \quad (4.1.110)$$

where  $e_{i,j}$  are Fourier coefficients,  $-N_x \leq i, n \leq N_x, -N_y \leq j, m \leq N_y$ ,

Since the form of systems of differential equations in two- and three-dimensional cases is identical, then the same and all subsequent changes are also identical. The system of differential equations for the vectors  $\mathbf{S}_x, \mathbf{S}_y, \mathbf{U}_x, \mathbf{U}_y$ , in (4.1.107) has the form (1.4.36)–(4.1.38). In particular, for the grating of an isotropic material, and when  $\varepsilon = (x, y)$  and  $\mu = 1$  are scalars, the matrix of the system of differential equations (4.1.36) has the form

$$\mathbf{A} = - \begin{bmatrix} \mathbf{0} & \mathbf{0} & \mathbf{K}_y \mathbf{E}^{-1} \mathbf{K}_x & \mathbf{I} - \mathbf{K}_y \mathbf{E}^{-1} \mathbf{K}_y \\ \mathbf{0} & \mathbf{0} & \mathbf{K}_x \mathbf{E}^{-1} \mathbf{K}_x - \mathbf{I} & -\mathbf{K}_x \mathbf{E}^{-1} \mathbf{K}_y \\ \mathbf{K}_y \mathbf{K}_x & \mathbf{E} - \mathbf{K}_y^2 & \mathbf{0} & \mathbf{0} \\ \mathbf{K}_x^2 - \mathbf{E} & -\mathbf{K}_x \mathbf{K}_y & \mathbf{0} & \mathbf{0} \end{bmatrix}, \quad (4.1.111)$$

where the matrix  $\mathbf{E}$  is given by (4.1.109) and is composed of the Fourier coefficients of functions  $\varepsilon(x, y)$ . Equation (4.1.111) can be obtained from the general expressions (1.4.37), (1.4.38) for

$$\begin{aligned}\mathbf{E}_{1,1} &= \mathbf{E}_{2,2} = \mathbf{E}_{3,3} = \mathbf{E}, \\ \mathbf{E}_{1,2} &= \mathbf{E}_{1,3} = \mathbf{E}_{2,1} = \mathbf{E}_{2,3} = \mathbf{E}_{3,1} = \mathbf{E}_{3,2} = \mathbf{0}, \\ \mathbf{M}_{1,1} &= \mathbf{M}_{2,2} = \mathbf{M}_{3,3} = \mathbf{I}, \\ \mathbf{M}_{1,2} &= \mathbf{M}_{1,3} = \mathbf{M}_{2,1} = \mathbf{M}_{2,3} = \mathbf{M}_{3,1} = \mathbf{M}_{3,2} = \mathbf{0}.\end{aligned}\tag{4.1.112}$$

Consider the transition to the space–frequency representation (4.1.107), using the correct rules of Fourier expansions of the products of functions. Derivation of formulas will be carried out for the case of an isotropic material. The system of Maxwell's equations (4.1.28) contains only the following three products:  $\varepsilon E_z$ ,  $\varepsilon E_x$ ,  $\varepsilon E_y$ .

The tangential component  $E_z$  is continuous, and therefore the product  $\varepsilon E_z$  is expanded into a Fourier series with the Laurent rules (4.1.42). In this case, the corresponding matrix  $E_{3,3}$  in (4.1.107) has the form (4.1.110).

We assume that the boundaries of two media with different dielectric constants in each layer are parallel to the coordinate axes [6]. Consider the product  $Dx = \varepsilon E_x$ . The product  $D_x$  is continuous at the sections of the interfaces parallel to the axis  $Oy$ . Indeed, at these sites  $D_x = \varepsilon E_x$  is a normal component of electric displacement. At the same time, the component  $E_x$  and the function of the dielectric constant  $\varepsilon$  are discontinuous at these boundaries. Thus, the product  $D_x = \varepsilon E_x$  is continuous in  $x$  for any fixed  $y$ . Accordingly, for the expansion of  $Dx = \varepsilon E_x$  into the Fourier series in the variable  $x$  we used the inverse Laurent rule (4.1.43)

$$d_{x,i}(y, z) = \sum_n \varepsilon_{x,i,n}(y) S_{x,n}(y, z),\tag{4.1.113}$$

where  $d_{x,i}(y, z)$ ,  $S_{x,n}(y, z)$  are the Fourier coefficients of the functions  $D_x$ ,  $\varepsilon E_x$ , and  $\varepsilon_{x,i,n}(y)$  are the elements of the Toeplitz matrix  $\llbracket 1/\varepsilon_x \rrbracket^{-1}$  formed from the Fourier coefficients with respect to variable  $x$  of the function  $1/\varepsilon(x, y)$ . In sections of the boundaries of the media parallel to the axis  $Ox$ , the component  $E_x$  is tangential and therefore continuous in  $y$ . The Fourier coefficients  $S_{x,n}(y, z)$  of function  $E_x$  are also continuous. Therefore, for the expansion in (4.1.113) of terms  $\varepsilon_{x,i,n}(y) S_{x,n}(y, z)$  into a Fourier series in  $y$  we apply the Laurent rule (4.1.42)

$$d_{x,i,j}(z) = \sum_{n,m} \varepsilon_{x,i,n,j-m} S_{x,n,m}(z),\tag{4.1.114}$$

where  $\varepsilon_{x,i,n,j-m}$  are the Fourier coefficients with the number  $(j-m)$  of the function  $\varepsilon_{x,i,n}(y)$ .

Repeating a similar argument for  $D_y = E_y$ , we obtain

$$d_{y,j}(x,z) = \sum_m \varepsilon_{y,j,m}(x) S_{y,m}(x,z), \quad (4.1.115)$$

$$d_{y,i,j}(z) = \sum_{n,m} \varepsilon_{y,i-n,j,m} S_{y,n,m}(z), \quad (4.1.116)$$

where  $\varepsilon_{y,j,m}(y)$  are the elements of the Toeplitz matrix  $\llbracket 1/\varepsilon_y \rrbracket^{-1}$  formed from the Fourier coefficients of the variable  $y$  of the function  $1/\varepsilon(x,y)$ , and  $\varepsilon_{y,i-n,j,m}$  is the Fourier coefficient with the number  $(i-n)$  of the function  $\varepsilon_{y,j,m}(x)$ .

Equations (4.1.114) and (4.1.116) were obtained using the correct rules of expansion into Fourier series of the products  $D_x = \varepsilon E_x$ ,  $D_y = \varepsilon E_y$ . Accordingly, in the transition from the system (1.4.28) to the space–frequency representation (4.1.107), the matrices  $\mathbf{E}_{1,1}$  and  $\mathbf{E}_{2,2}$  will have the form

$$\begin{aligned} E_{1,1} l(i,n), l(j,m) &= \varepsilon_{x,i,n,j-m}, \\ E_{2,2} l(i,n), l(j,m) &= \varepsilon_{y,i-n,j,m}, \end{aligned} \quad (4.1.117)$$

where  $l(i,j)$  is defined in (4.1.108),  $-N_x \leq i, n \leq N_x$ ,  $-N_y \leq j, m \leq N_y$ . Matrices in (4.1.117) have dimension  $(2N_x+1)(2N_y+1) \times (2N_x+1)(2N_y+1)$ .

As a result, the matrix  $\mathbf{A}$  of the system of linear differential equations takes the form:

$$\mathbf{A} = - \begin{bmatrix} \mathbf{0} & \mathbf{0} & \mathbf{K}_y \mathbf{E}^{-1} \mathbf{K}_x & \mathbf{I} - \mathbf{K}_y \mathbf{E}^{-1} \mathbf{K}_y \\ \mathbf{0} & \mathbf{0} & \mathbf{K}_x \mathbf{E}^{-1} \mathbf{K}_x - \mathbf{I} & -\mathbf{K}_x \mathbf{E}^{-1} \mathbf{K}_y \\ \mathbf{K}_y \mathbf{K}_x & \mathbf{E}_{1,1} - \mathbf{K}_y^2 & \mathbf{0} & \mathbf{0} \\ \mathbf{K}_x^2 - \mathbf{E}_{2,2} & -\mathbf{K}_x \mathbf{K}_y & \mathbf{0} & \mathbf{0} \end{bmatrix}. \quad (4.1.118)$$

Detailed description of the correct rules of expansion into a Fourier series for the general case of the tensors of dielectric permittivity and magnetic permeability can be found in [8, 9].

Subsequent operations on the ‘cross-linking’ of solutions at the layer boundaries and numerically stable implementation of the calculation of the matrix of the system of linear equations for the amplitudes of the diffraction orders are also the same. Matrices  $\mathbf{E}$ ,  $\mathbf{F}$  in the systems of linear equations that represent the tangential field components (4.1.102), (4.1.103) on the upper and lower boundaries of the lattice also have the form (4.1.76), (4.1.77), where

$$\begin{aligned} \sin \Phi &= \text{diag}_{l(i,j)} \frac{k_{y,j}}{\sqrt{k_{x,i}^2 + k_{y,j}^2}}, \quad \cos \Phi = \text{diag}_{l(i,j)} \frac{k_{x,i}}{\sqrt{k_{x,i}^2 + k_{y,j}^2}}, \\ \cos \Theta^{(1)} &= \text{diag}_{l(i,j)} \frac{-k_{z,1,i,j}}{k_0 n_1^2}, \quad \cos \Theta^{(2)} = \text{diag}_{l(i,j)} \frac{k_{z,2,i,j}}{k_0 n_2^2}, \end{aligned} \quad (4.1.119)$$

$\text{diag} f(i, j)$  denotes the diagonal matrix composed of elements  $f(i, j)$ , arranged in the ascending order of magnitude  $l(i, j)$ .

#### 4.1.4. Examples of calculation of diffraction gratings

The method of Fourier modes can be used to calculate a wide class of periodic structures, including beam splitters, polarizers, antireflection structures, etc. In this section we consider several typical examples of these devices.

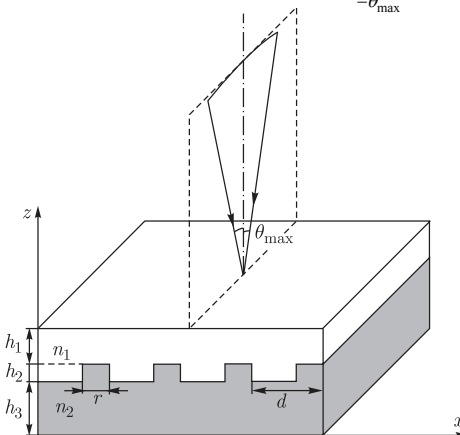
##### 4.1.4.1. Gratings–polarizers

Figure 4.1.2 shows the geometry of the grating–polarizer (period  $d$ ), intended for the transmission of the component of the incident wave with TM-polarization and reflection of the component with TE-polarization. Such gratings are of great practical importance in systems for illumination of LCD monitors.

The grating in Fig. 4.1.2 has the properties of the polarizer with at incidence of a wave when the projection of the vector of direction of the incident wave on the grating plane is parallel to the axis  $Oy$  (when  $\phi = \pi/2$  in (4.1.24)). Figure 4.1.2 schematically shows the directions of the incident wave in this geometry for the symmetric range of angles  $\theta \in [-\theta_{\max}, \theta_{\max}]$ .

Calculation of the geometric parameters of the structure in Fig.4.1.2 was carried out using a gradient optimization procedure [20] at the wavelength  $\lambda = 550$  nm and the refractive index of materials  $n_1 = 1.5$ ,  $n_2 = 1.72$ . In practice, the structure should have polarizing properties for a certain range of incidence angles  $\theta \in [-\theta_{\max}, \theta_{\max}]$ . Therefore, as the target function we select the following integral criterion

$$\varepsilon(h_1, h_2, h_3, d, r) = \int_{-\theta_{\max}}^{\theta_{\max}} (T_{\text{TM}}(\theta) - T_{\text{TE}}(\theta)) d\theta \rightarrow \max, \quad (4.1.120)$$



**Fig. 4.1.2.** Geometry of the grating-polarizer geometry and incident wave.

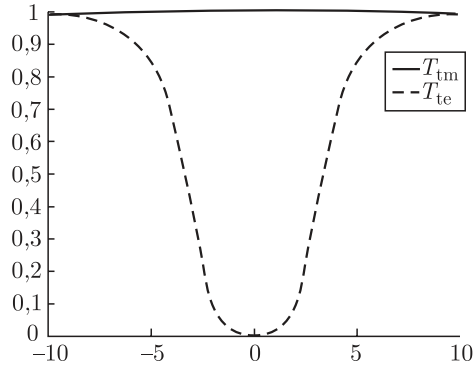


**Fig. 4.1.3.** The transmission of structure depending on the angle of incidence with the incident wave with TM-polarization (solid line) and TE-polarized (dashed line).

where  $T_{TM}(\theta)$ ,  $T_{TE}(\theta)$  is the intensity of the transmitted zero diffraction orders with incident waves with TM-polarization ( $\mathbf{H} = (H_x, 0, 0)$ ,  $\mathbf{E} = (0, E_y, E_z)$ ) and the TE-polarization ( $\mathbf{E} = (E_x, 0, 0)$ ,  $\mathbf{H} = (0, H_y, H_z)$ ), respectively. The calculation  $T_{TM}(\theta)$ ,  $T_{TE}(\theta)$  in (4.1.120) is carried out by the method of Fourier modes. As a result, optimization at  $\theta_{\max} = 2^\circ$  yielded the following parameters: period  $d = 482$  nm,  $h_1 = 205$  nm,  $h_2 = 285$  nm,  $h_3 = 998$  nm,  $r = 233$  nm. Figure 4.1.3 shows the calculated transmission of graphics structures, depending on the angle of incidence with the incident waves with TM polarization and the TE polarization. Figure 4.1.3 shows that the calculated structure in the required range of angles completely transmits the emission with TM-polarization. The transmission for a wave with TE-polarization is zero at normal incidence and is less than 10% at  $\theta \in [-2^\circ, 2^\circ]$ . When using the grating in Fig. 4.1.2a it is difficult to achieve good polarization properties at  $\theta_{\max} > 2^\circ$ . The polarization properties in a large angular range can be achieved using a sandwich-type structure obtained by repeating the grating in Fig. 4.1.2a on the axis  $Oz$ . In this case the vertical periods of the sandwich structure are identical and have the form shown in Fig. 4.1.2.

We calculated the structure containing four vertical periods for the interval of angles of incidence  $\theta \in [-10^\circ, 10^\circ]$ . Optimization of the function (4.1.120) at  $\theta_{\max} = 10^\circ$  resulted in the following parameters: period  $d = 439$  nm,  $h_1 = 38$  nm,  $h_2 = 460$  nm,  $r = 287$  nm. Calculated transmission graphs for a structure with four vertical periods are shown in Fig. 4.1.4.

Figure 4.1.4 shows that the calculated structure in the angular range  $\theta \in [-10^\circ, 10^\circ]$  is the transmission coefficient for a wave with TM-polarization above 97%. In this case the transmission for a wave with TE-polarization does not exceed 10%, and at  $\theta \in [-5^\circ, 5^\circ]$  it is less than 1.5%.

#### 4.1.4.2. The beam splitter

Gratings are widely used as beam splitters. Binary diffraction gratings are the easiest to manufacture. The binary grating contains at period  $K$  rectangular lines

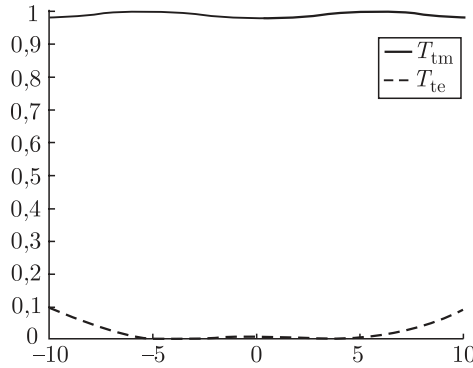


**Fig. 4.1.4.** The transmission of a structure with four vertical periods, depending on the angle of incidence with the incident wave with TM-polarization (solid line) and TE-polarization (dashed line)/

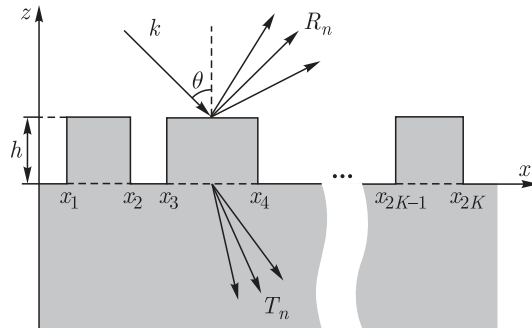


**Fig. 4.1.5.** Geometry of a binary dielectric grating.

of the same height but different widths (see Fig. 4.1.5). The task of calculating the beam splitter is formulated as the problem of calculating the coordinates of the profile lines  $x_1, \dots, x_{2K}$  and the height of the lines  $a$  is formulated from the conditions of formation of the given intensities of the diffraction orders. Depending on the type of grating (dielectric, metallic, or impermeable, reflecting) the profile is calculated from the condition of the formation of given intensities of reflected or transmitted diffraction orders [20].

The method of Fourier modes was used for the calculation of binary dielectric gratings with equal intensity of transmitted  $2N + 1$  orders. Order numbers are symmetrical, from  $-N$  to  $N$ . Calculation of grating parameters  $\mathbf{p} = (x_1, \dots, x_{2K}, a)$  was performed using the gradient optimization procedure [20] at the period  $d = 5.5 \lambda$ , at normal incidence of the wave ( $\theta = 0$ ) and at the refractive indices of the grating material and the substrate  $n = 1.5$ . The target function was the quadratic error function

$$\varepsilon(\mathbf{p}) = \sum_{j=-N}^N (I_j^T(\mathbf{p}) - I)^2 \rightarrow \min, \tag{4.1.121}$$

**Table 4.1.1.** The results of calculation of binary dielectric gratings in electromagnetic theory ( $d = 5.5\lambda$ ,  $n = 1.5$ ,  $\theta = 0$ )

Number of orders $2N+1$	Number of lines $K$	Height of lines $(a/\lambda)$	Coordinates of the profile	$E$ , (%)	$\delta$ (%)
<b>TM-polarization</b>					
3	1	0.675	(0.283, 0.7719)	80.1	3.1
5	2	0.9	(0.1800, 0.4841), (0.5525, 0.8567)	80.1	3.1
7	2	0.885	(0.2392, 0.4447) (0.5919, 0.7974)	87.7	0.34
9	3	1.7	(0.1000, 0.1924) (0.3842, 0.4777) (0.6217, 0.7154)	94.6	1.6
11	3	1.61	(0.1542, 0.3454), (0.4858, 0.5729), (0.713, 0.9043)	94.4	6.9
<b>TE-polarization</b>					
3	1	0.65	(0, 0.5)	85	0.005
5	2	0.9	(0.1832, 0.4785), (0.5579, 0.8535)	80.2	0.08
7	2	0.875	(0.2584, 0.4296), (0.6067, 0.7779)	83.8	0.7
9	3	1.0	(0.0117, 0.1945), (0.3198, 0.4838), (0.7819, 0.9545)	89.4	3.6
11	3	1.57	(0.0446, 0.3383), (0.5049, 0.556), (0.8268, 0.8779)	90.7	5.6

where  $I_j^T(\mathbf{p})$  is the intensity of transmitted orders. The results of calculations of the gratings are given in Table 4.1.1 for TE- and TM-polarization of the incident wave. In the last two columns of the table there are the values of energy efficiency

$$E = \sum_{j=-N}^N I_j \quad (4.1.122)$$

and the standard error of formation of the given equal intensity of the orders

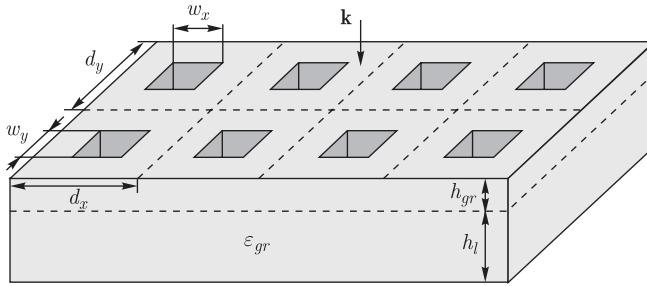
$$\delta = \frac{1}{\bar{I}} \left[ \frac{1}{2N+1} \sum_{j=-N}^N (I_j - \bar{I})^2 \right]^{\frac{1}{2}}, \quad (4.1.123)$$

where  $\bar{I} = E / (2N+1)$  is the average intensity. The coordinates of the profile in Table 4.1.1 are normalized to the value of the period.

The calculation results show the possibility of formation of 5–11 equal orders at the energy efficiency of 80–90% and a low rms error. Note that the methods of the scalar theory can not be used in the calculation of diffraction gratings with the specified period [20].

**Table 4.1.2.** The intensity of the order of three-dimensional binary lattice

Indices of orders ( $i, j$ )	-1	0	+1
-1	0.0881	0.0885	0.0879
0	0.0885	0.0875	0.0885
+1	0.0879	0.0885	0.0881

**Fig. 4.1.6.** Geometry of the dielectric binary grating

Three-dimensional binary diffraction gratings are used to generate the required two-dimensional set of diffraction orders. The method of Fourier modes was used to calculate a three-dimensional binary dielectric grating to form nine equal intensity orders with numbers  $(i, j)$ ,  $i, j = -1, 0, 1$ . In this case, it suffices to use a simple binary grating having a rectangular recess at one period (Fig. 4.1.6). Calculation of structural parameters was performed at a wavelength  $\lambda = 808$  nm, equal periods  $d_x = d_y = d = 2362$  nm, the refraction index of the grating material  $n = \sqrt{\epsilon_{gr}} = 1.54$  for the case of normally incident waves with the angle of polarization  $\psi = 45^\circ$ . In this case, the electric vector of the incident wave coincides with the bisector of the 1st quadrant. The geometrical parameters of the structure  $h_{gr} = 1955$  nm,  $w_x = 0.9d$  were determined using the gradient optimization procedure. In the calculations it was assumed that the total thickness of the grating  $h_{gr} + h_l$  is 0.6 mm.

The calculated values of intensities of the orders of the grating at the given parameters are given in Table. 4.1.2. Table 4.1.2 shows the high uniformity of intensity distribution in the orders, the mean square error of (4.1.123) is less than 1%. The energy efficiency of the grating is 79.4%.

#### 4.1.4.3. Subwavelength antireflection coatings

The method of Fourier modes was used for the calculation of binary subwavelength antireflection gratings. The term ‘subwavelength grating’ means that the grating has only zero reflected and transmitted propagating orders. The remaining orders correspond to evanescent waves. For the existence of only zero order at normal incidence, the periods of the grating must satisfy the condition  $d_x, d_y < \lambda / \sqrt{\epsilon_{gr}}$ .

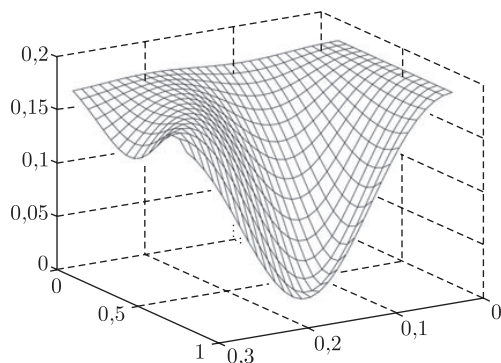


**Fig. 4.1.7.** The dependence of the reflection coefficient  $I_{00}^R$  on the depth  $h/\lambda \in (0, 0.3)$  and the of the side of a square recess  $w/d \in (0.1, 0.8)$ .

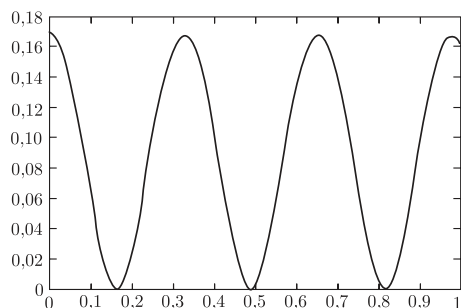


**Fig. 4.1.8.** The dependence of the reflection coefficient  $I_{00}^R$  on the depth ( $h/\lambda$ ) at the optimum size of the side of the recess  $w/d = 0.8$ .

The antireflective coating was a simple binary grating with equal periods  $d_x = d_y = d$ , as shown in Fig. 4.1.6. Calculations of the antireflective coating consisted of calculating the intensity of the zero reflected order  $I_{00}^R$  at different depths of the recess  $h_{\text{gr}}$  and the size of the recess  $w_x = w_y = w$  for a fixed period  $d$ . The values  $h_{\text{gr}}$ ,  $w$ , ensuring minimum reflection  $I_{00}^R$  are also optimized grating parameters.

The following parameters were chosen for calculations:  $\lambda = 10.6 \mu\text{m}$ ,  $\varepsilon_{\text{gr}} = 5.76$ ,  $d = 0.25 \lambda = 2.65 \mu\text{m}$ . These values of permittivity  $\varepsilon_s$  and wavelength correspond to the case of synthesis of the antireflective coating of ZnSe (zinc selenide) for a  $\text{CO}_2$  laser. The problem of synthesis of such coatings is especially important for high-power  $\text{CO}_2$  lasers. Figure 4.1.7 shows a graph of the function  $I_{00}^R(h, r, d)$  at  $h \in (0, 3.5) \mu\text{m}$  and  $w/d \in (0.1, 0.8)$ . The calculation was performed for a normal incidence plane wave. The incident wave was represented by a superposition of  $E$ - and  $H$ -waves with equal coefficients. Such a representation simulates the case of unpolarized light.

Figure 4.1.7 shows that at  $w/d \approx 0.8$  and  $h_{\text{gr}} \approx 1.8 \mu\text{m}$  there is a pronounced minimum reflection coefficient  $I_{00}^R(h, r, d)$ . Figure 4.1.8 shows a plot of the reflection coefficient  $I_{00}^R(h, r, d)$  at the optimal size of the recess  $w = 0.8d$  and

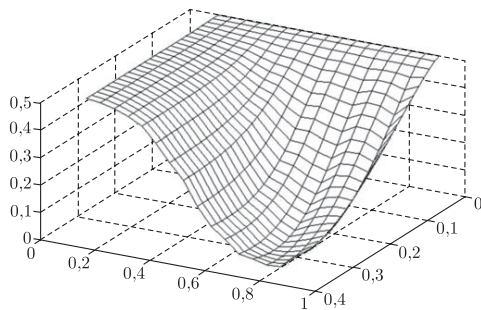


**Fig. 4.1.9.** The dependence of the reflection coefficient of the depth  $h/\lambda \in (0, 0.4)$  and the size of the recess  $w/d \in (0, 1.0.9)$ .

different heights. From the graph in Fig 4.1.8 one can see that the reflection coefficient decreases to zero at the depths  $0.18\lambda$ ,  $0.49\lambda$  and  $0.82\lambda$ . Thus, on a plane zinc selenide – air interface the reflection coefficient is approximately 17%

Investigations were carried out into the possibility of using the simplest binary gratings (Fig. 4.1.6) as a reflective coating for tungsten in the visible spectrum at  $\lambda = 0.55 \mu\text{m}$ . In this case, the dielectric constant is complex and  $\lambda = 0.55 \mu\text{m}$   $\epsilon_{\text{gr}} = 4.8 + 19.11i$ . The graph of the reflection coefficient  $I_{00}^R(h, r, d)$  for a tungsten binary grating with the period  $d = 0.85\lambda$  is shown in Fig. 4.1.9. Figure 4.1.9 shows that the minimum reflection coefficient is achieved when the size of the recess is  $w/d \approx 0.75$  and depth  $h_{\text{gr}} \approx 0.35$ .

The graph of the reflection coefficient at the optimum size of the recess is shown in Fig. 4.1.10. The graph shows that the reflection coefficient for a plane tungsten–air boundary is close to 50%. With increasing depth the reflection coefficient decreases, reaching zero at depth  $h_{\text{gr}} = 0.33\lambda$ . In contrast to dielectric gratings (Fig. 4.1.8), the secondary minima are not very pronounced. Figure 4.1.11 shows a graph for the reflection coefficient at the optimum size of the recess, depending on the wavelength range from  $0.35 \mu\text{m}$  to  $3.5 \mu\text{m}$ . The top graph in Fig. 4.1.11 shows the reflection

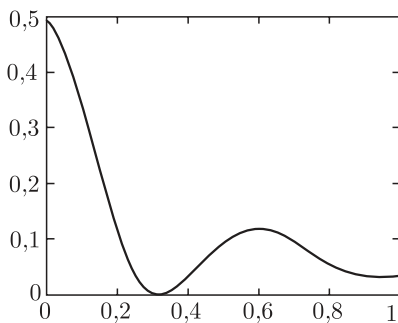


**Fig. 4.1.10.** Dependence of the reflection coefficient of the depth ( $h/\lambda$ ) at the optimal size of the recess  $w/d = 0.75$ .

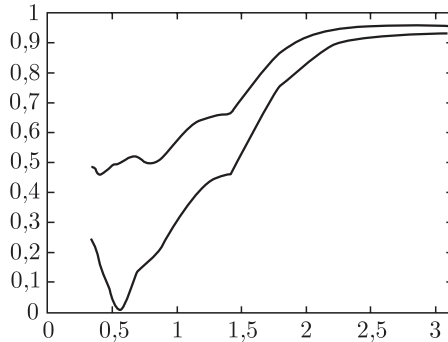


**Fig. 4.1.11.** Dependence of the reflection coefficient on wavelength  $w/d = 0.75$ ,  $h_{gr} = 0.33$

coefficient for a planar tungsten–air interface. Figure 4.1.11 shows the presence of a sharp minimum of the reflection coefficient near the calculated wavelength  $\lambda = 0.55 \mu\text{m}$ . At the same time across the entire visible range the reflection coefficient for a binary grating is half the coefficient than for the planar interface.

## 4.2. Formation of high-frequency interference patterns of surface electromagnetic waves by diffraction gratings

Due to diffraction, the light can not be focused to a small spot. The minimum diameter of the spot is about half a wavelength. Thus, in the best diffraction-limited microscopy systems the maximum attainable resolution is of the order of hundreds of nanometers. Using the interference patterns of surface electromagnetic waves (SEW) we can achieve superresolution of about a tenth of a wavelength of the light used.

In section 2.1 we derive the equations of SEW from Maxwell's equations and examine the characteristics of the SEW. Section 2.1.3 examines the Kretschmann scheme for SEW excitation and the formation of interference patterns in the framework of the scheme.

The paragraphs 2.2 and 2.3 discuss the formation of interference patterns of the SEW with a diffraction structure consisting of a dielectric diffraction grating (one- or two-dimensional) and a metal film placed under the grating in the region of the substrate [21–25]. Diffraction gratings are used for excitation at the lower surface of the metal film of a given set of SEW, which form an interference pattern. The excitation of SEW and the formation of interference patterns are carried out using higher diffraction orders (with numbers  $\pm m$ ,  $m > 1$ ). This allows to generate high-frequency interference patterns with a period several times smaller than the wavelength of incident light with a low-frequency diffraction microrelief with a period several times greater than the wavelength of incident radiation [21–24]. These diffraction structures are used in surface plasmon interference nanolithography). In this case the interference pattern of SEW is recorded in the resist, which is located directly below the metal film and then the appropriate nano- or microstructure is

produced [26–30]. When using electron beam lithography for the production of a similar structure with a substantially subwavelength period the required sample screen size (resolution) should not be more than a quarter period of the interference pattern. Using the interference patterns of the SEW we can achieve resolution of a few tens of nanometers (about a tenth of a wavelength).

Section 2.4 describes the integral representation of the electromagnetic field at the interface of two media through the angular spectrum of SEW and also describes the calculations of the diffraction structures for the transformation and focusing of the SEW. The calculation of the diffraction structures is based on the phase modulation of SEW, formed during the passage of a wave through the dielectric block, situated directly on the surface of propagation of SEW. The given phase modulation takes place both as a result of the variation of the height of the block above the surface at the fixed length and as a result of the change of the length of the block at the fixed height. The calculation of the ‘lens’ of surface electromagnetic waves is discussed as an example.

### 4.2.1. Surface electromagnetic waves (SEW)

#### 4.2.1.1. The equation of a surface electromagnetic wave

Consider the derivation of the equation of the surface electromagnetic wave (SEW) at the interface between two semi-infinite media from Maxwell’s equations. Let the interface be the plane  $z = 0$ , with the media 1 and 2 corresponding to the regions  $z > 0$  and  $z < 0$ , respectively.

We write a general representation of the field in the media 1 and 2. The index of the number of the medium in the field components and dielectric constants will be introduced later, before applying the boundary conditions at the interface. Since the properties of the medium do not depend on the variables  $x, y$ , then the electric and magnetic fields in the media 1 and 2 have the form

$$\begin{aligned}\mathbf{E}(x, y, z) &= \mathbf{E}(z) \exp(ik_0(\alpha x + \beta y)), \\ \mathbf{H}(x, y, z) &= \mathbf{H}(z) \exp(ik_0(\alpha x + \beta y)),\end{aligned}\tag{4.2.124}$$

where  $k_0 = 2\pi/\lambda$ ,  $\lambda$  is the wavelength in vacuum. Substituting (4.2.1) into Maxwell’s equations for a monochromatic field (4.1.3), we obtain:

$$\begin{aligned}ik_0\beta H_z - \frac{\partial H_y}{\partial z} &= -ik_0\varepsilon E_x, & ik_0\beta E_z - \frac{\partial E_y}{\partial z} &= ik_0H_x, \\ \frac{\partial H_x}{\partial z} - ik_0\alpha H_z &= -ik_0\varepsilon E_y, & \frac{\partial E_x}{\partial z} - ik_0\alpha E_z &= ik_0H_y, \\ ik_0\alpha H_y - ik_0\beta H_x &= -ik_0\varepsilon E_z, & ik_0\alpha E_y - ik_0\beta E_x &= ik_0H_z.\end{aligned}\tag{4.2.125}$$

We rewrite equation (4.2.125) in the form of

$$E_x = \frac{1}{ik_0(\varepsilon - \beta^2)} \left( \frac{\partial H_y}{\partial z} - ik_0 \alpha \beta E_y \right), \quad (4.2.126)$$

$$H_x = \frac{-1}{ik_0(\varepsilon - \beta^2)} \left( \varepsilon \frac{\partial E_y}{\partial z} + ik_0 \alpha \beta H_y \right),$$

$$E_z = \frac{-1}{ik_0(\varepsilon - \beta^2)} \left( \beta \frac{\partial E_y}{\partial z} + ik_0 \alpha H_y \right), \quad (4.2.127)$$

$$H_z = \frac{1}{ik_0(\varepsilon - \beta^2)} \left( ik_0 \varepsilon \alpha E_y - \beta \frac{\partial H_y}{\partial z} \right),$$

where the components  $E_y$  and  $H_y$  satisfy the Helmholtz equation:

$$\begin{aligned} \frac{\partial^2 E_y}{\partial z^2} + k_0^2 (\varepsilon - \alpha^2 - \beta^2) E_y &= 0, \\ \frac{\partial^2 H_y}{\partial z^2} + k_0^2 (\varepsilon - \alpha^2 - \beta^2) H_y &= 0. \end{aligned} \quad (4.2.128)$$

Solving (4.2.5), we obtain equations for the components  $E_y$  and  $H_y$  in the media 1 and 2:

$$\begin{aligned} E_y^{(1)}(x, y, z) &= e_1 \exp(ik_0(\alpha x + \beta y)) \exp(-k_0 \gamma_1 z), \\ H_y^{(1)}(x, y, z) &= h_1 \exp(ik_0(\alpha x + \beta y)) \exp(-k_0 \gamma_1 z), \\ E_y^{(2)}(x, y, z) &= e_2 \exp(ik_0(\alpha x + \beta y)) \exp(k_0 \gamma_2 z), \\ H_y^{(2)}(x, y, z) &= h_2 \exp(ik_0(\alpha x + \beta y)) \exp(k_0 \gamma_2 z), \end{aligned} \quad (4.2.129)$$

where

$$\gamma_i^2 = \alpha^2 + \beta^2 - \varepsilon_i, \quad (4.2.130)$$

index  $i = 1, 2$  indicates the number of the medium,  $e_i, h_i$  are arbitrary constants. Representation of the field (4.2.6) corresponds to the SEW because it is fading in the direction  $z$ , perpendicular to the interface.

Substituting (4.2.6) into (4.2.3) we get a second pair of tangential components  $E_x$  and  $H_x$  in the form

$$\begin{aligned}
E_x^{(1)} &= \frac{-1}{i(\varepsilon_1 - \beta^2)} (h_1 \gamma_1 + e_1 i \alpha \beta) \exp(ik_0(\alpha x + \beta y)) \exp(-k_0 \gamma_1 z), \\
H_x^{(1)} &= \frac{-1}{i(\varepsilon_1 - \beta^2)} (-e_1 \varepsilon_1 \gamma_1 + h_1 i \alpha \beta) \exp(ik_0(\alpha x + \beta y)) \exp(-k_0 \gamma_1 z), \\
E_x^{(2)} &= \frac{1}{i(\varepsilon_2 - \beta^2)} (h_2 \gamma_2 - e_2 i \alpha \beta) \exp(ik_0(\alpha x + \beta y)) \exp(k_0 \gamma_2 z), \\
H_x^{(2)} &= \frac{-1}{i(\varepsilon_2 - \beta^2)} (e_2 \varepsilon_2 \gamma_2 + h_2 i \alpha \beta) \exp(ik_0(\alpha x + \beta y)) \exp(k_0 \gamma_2 z).
\end{aligned} \tag{4.2.131}$$

We write the conditions of equality of the tangential components of electric and magnetic fields at the interface of the media at  $z = 0$ :

$$\begin{cases}
E_y^{(1)}(x, y, 0) = E_y^{(2)}(x, y, 0), \\
H_y^{(1)}(x, y, 0) = H_y^{(2)}(x, y, 0), \\
E_x^{(1)}(x, y, 0) = E_x^{(2)}(x, y, 0), \\
H_x^{(1)}(x, y, 0) = H_x^{(2)}(x, y, 0).
\end{cases} \tag{4.2.132}$$

From the first two equations in (4.2.9) we obtain

$$e_1 = e_2, \quad h_1 = h_2. \tag{4.2.133}$$

Substituting (4.2.131), (4.2.133) into the second two equations of (4.2.9), we have:

$$\begin{cases}
e_1 \left( \frac{\varepsilon_1 \gamma_1}{\varepsilon_1 - \beta^2} + \frac{\varepsilon_2 \gamma_2}{\varepsilon_2 - \beta^2} \right) + h_1 \left( \frac{i \alpha \beta}{\varepsilon_2 - \beta^2} - \frac{i \alpha \beta}{\varepsilon_1 - \beta^2} \right) = 0, \\
e_1 \left( \frac{i \alpha \beta}{\varepsilon_1 - \beta^2} - \frac{i \alpha \beta}{\varepsilon_2 - \beta^2} \right) + h_1 \left( \frac{\gamma_1}{\varepsilon_1 - \beta^2} + \frac{\gamma_2}{\varepsilon_2 - \beta^2} \right) = 0.
\end{cases} \tag{4.2.134}$$

A non-trivial solution of (4.2.11) will exist when the determinant of system (4.2.11) is zero. Thus, we obtain

$$\left( \frac{\gamma_1}{\varepsilon_1 - \beta^2} + \frac{\gamma_2}{\varepsilon_2 - \beta^2} \right) \left( \frac{\varepsilon_1 \gamma_1}{\varepsilon_1 - \beta^2} + \frac{\varepsilon_2 \gamma_2}{\varepsilon_2 - \beta^2} \right) - \alpha^2 \beta^2 \left( \frac{1}{\varepsilon_1 - \beta^2} - \frac{1}{\varepsilon_2 - \beta^2} \right)^2 = 0. \tag{4.2.135}$$

A direct substitution shows that equation (4.2.12) becomes an identity when the following condition is fulfilled

$$k_0^2 (\alpha^2 + \beta^2) = k_0^2 \frac{\varepsilon_1 \varepsilon_2}{\varepsilon_1 + \varepsilon_2}. \quad (4.2.136)$$

Equation (4.2.136) is the dispersion equation of SEW. Under the condition (4.2.13) component  $H_z$  in (4.2.127) is identically zero. Thus, the vector  $\mathbf{H}$  at the SEW is situated in the plane of the interface between two media.

Direct analysis shows that the fields in the equations (4.2.6) and (4.2.8) have the damping form with respect to  $z$  under the condition  $\text{Re}(\varepsilon_1 + \varepsilon_2) < 0$ . This condition can occur at the interface between metal and dielectric. The dielectric constant of metals with high conductivity has a large negative real part and a small imaginary part, which ensures the fulfillment of the above conditions. For convenience, we replace the indices 1 and 2, denoting the number of the medium, by the indices  $m$  and  $d$  denoting the metal and the dielectric, respectively, and introduce the quantity

$$k_{\text{SPP}} = k_0 \sqrt{\frac{\varepsilon_m \varepsilon_d}{\varepsilon_m + \varepsilon_d}}. \quad (4.2.137)$$

Quantity  $k_{\text{SPP}}$  is called the constant of propagation of SEW and determines the projection of the wave vector of the SEW on the plane  $xOy$ .

In a particular case  $\beta = 0$  we obtain the SEW propagating along the axis  $Ox$ . In this case, equation (4.2.12) takes the form

$$\left( \frac{\gamma_1}{\varepsilon_1} + \frac{\gamma_2}{\varepsilon_2} \right) (\gamma_1 + \gamma_2) = 0,$$

which immediately yields the dispersion equation  $k_0^2 \alpha^2 = k_{\text{SPP}}^2$ . Note that at  $\beta = 0$  from (4.2.134) it follows that  $e_1 = 0$ . Thus, from (4.2.129) and (4.2.131) we have:

$$\mathbf{E}^{(i)} = (E_x^{(i)}, 0, E_z^{(i)}), \quad \mathbf{H}^{(i)} = (0, H_y^{(i)}, 0), \quad i = 1, 2. \quad (4.2.138)$$

The expressions (4.2.138) show that the SEWs propagating along the axis  $Ox$ , are TM-polarized.

It should be noted that the value  $k_{\text{SPP}}$  is complex, since the dielectric constant  $\varepsilon_m$  is complex:

$$\varepsilon_m = \varepsilon_m' + i\varepsilon_m''. \quad (4.2.139)$$

Thus, the SEW decays also in the direction of propagation. Note that since  $\varepsilon_m'' < 0$  then the inequality

$$\left| \sqrt{\frac{\varepsilon_m}{\varepsilon_m + \varepsilon_d}} \right| > 1. \quad (4.2.140)$$

is fulfilled. According to (4.2.140), we obtain

$$|k_{\text{SPP}}| > \sqrt{\varepsilon_d} k_0. \quad (4.2.141)$$

Inequality (4.2.141) shows that for excitation of the SEW we can not use a plane wave incident on a medium with permittivity  $\varepsilon_d$ . SEWs are excited using special optical circuits containing a prism made of a material with higher dielectric constant or diffraction gratings.

#### 4.2.1.2. The properties of surface electromagnetic waves

To characterize the SEW, we use quantities such as the wavelength, the propagation length, the depth of penetration into the dielectric and metallic media [31]. For convenience,  $k_{\text{SPP}}$  is presented in the form

$$k_{\text{SPP}} = k'_{\text{SPP}} + ik''_{\text{SPP}}, \quad (4.2.142)$$

where  $k'_{\text{SPP}}$  and  $k''_{\text{SPP}}$  are the real and imaginary parts, respectively.

The sections 2.2 and 2.3 of this chapter discuss the SEW on the border between silver and a dielectric with  $\varepsilon_d = 2.56$ . Accordingly, the characteristics of the SEW will be given for this pair of materials. The dependence of the dielectric constant of silver on the wavelength is shown in Fig. 4.2.1. At  $\lambda > 368$  nm  $\text{Re}(\varepsilon_m) + \varepsilon_d < 0$  and hence for such values of wavelength the SEW can exist at the interface.

The length of SEW is determined from the expressions

$$\lambda_{\text{SPP}} = 2\pi / k'_{\text{SPP}} = \lambda / \text{Re} \left( \sqrt{\frac{\varepsilon_m \varepsilon_d}{\varepsilon_m + \varepsilon_d}} \right). \quad (4.2.143)$$

In the case where the condition

$$|\varepsilon'_m + \varepsilon_d| \gg |\varepsilon''_m|, \quad (4.2.144)$$

an approximate expression holds

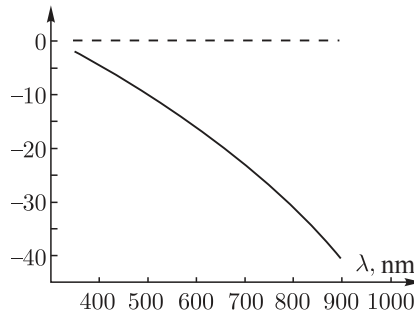


**Fig. 4.2.1.** The dependence of the dielectric constant of silver on the wavelength (the real part – solid line, imaginary part – dotted line).

$$k'_{\text{SPP}} \approx k_0 \sqrt{\frac{\varepsilon'_m \varepsilon_d}{\varepsilon'_m + \varepsilon_d}}. \quad (4.2.145)$$

In view of (4.2.145) we obtain an approximate expression for the length of SEW:

$$\lambda_{\text{SPP}} \approx \lambda \sqrt{\frac{\varepsilon'_m + \varepsilon_d}{\varepsilon'_m \varepsilon_d}}. \quad (4.2.146)$$

The normalized length of the SEW is defined by

$$\frac{\lambda_{\text{SPP}}}{\lambda} = 1 / \text{Re} \left( \sqrt{\frac{\varepsilon'_m \varepsilon_d}{\varepsilon'_m + \varepsilon_d}} \right). \quad (4.2.147)$$

When the condition (2.4.21) is fulfilled

$$\frac{\lambda_{\text{SPP}}}{\lambda} \approx \sqrt{\frac{\varepsilon'_m + \varepsilon_d}{\varepsilon'_m \varepsilon_d}}. \quad (4.2.148)$$

Since  $\varepsilon'_m < 0$  then, according to (4.2.23), we obtain

$$\lambda_{\text{SPP}} < \lambda. \quad (4.2.149)$$

This fact is the basis for the use of SEW in photolithography systems in the formation of nanostructures with subwavelength dimensions.

Figure 4.2.2 shows the dependence of the real (solid line) and imaginary (dashed line) parts of the value  $k_{\text{SPP}}/k_0$  on the wavelength, and Fig. 4.2.3 is the same graph for the normalized length of SEW. It is easy to see that the extrema of these quantities are obtained under the condition

$$\varepsilon'_m = -\varepsilon_d. \quad (4.2.150)$$

Condition (4.2.150) holds for  $\lambda \approx 368$  nm. The wavelength at which the condition (4.2.150) is fulfilled is called the resonance wavelength [28, 31]. Note that in the

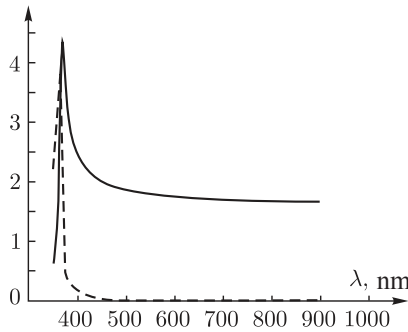


**Fig. 4.2.2.** The dependence of the normalized propagation constants of the SEW on the wavelength (the real part – solid line, imaginary part – dashed line).

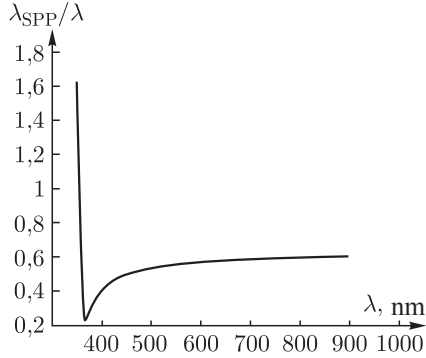


**Fig. 4.2.3.** The dependence of the normalized length of the wavelength of the SEW.

vicinity of the resonance wavelength the imaginary part of magnitude  $k_{\text{SPP}}/k_0$  also increases. As shown below, this leads to a decrease in the length of distribution of the SEW.

The SEW propagation length

$$\delta_{\text{SPP}} = \frac{1}{2k_{\text{SPP}}''}. \quad (4.2.151)$$

is defined as the distance at which the intensity of the wave decreases  $e$  times. When the condition (4.4.144) is fulfilled, the approximate equality holds

$$k_{\text{SPP}}'' \approx k_0 \frac{\varepsilon_m''}{2(\varepsilon_m')^2} \left( \frac{\varepsilon_m' \varepsilon_d}{\varepsilon_m' + \varepsilon_d} \right)^{\frac{3}{2}}. \quad (4.2.152)$$

Substituting (4.2.152) into (4.2.151), we obtain an approximate expression for the length of the SEW propagation in the form:

$$\delta_{\text{SPP}} \approx \lambda \frac{(\varepsilon_m')^2}{2\pi\varepsilon_m''} \left( \frac{\varepsilon_m' + \varepsilon_d}{\varepsilon_m' \varepsilon_d} \right)^{\frac{3}{2}}. \quad (4.2.153)$$

When the condition

$$|\varepsilon_m'| \gg |\varepsilon_d| \quad (4.2.154)$$

is fulfilled, we can write a simple approximate expression for:

$$\delta_{\text{SPP}} \approx \lambda \frac{(\varepsilon_m')^2}{2\pi\varepsilon_m''}. \quad (4.2.155)$$

Equation (4.2.155) shows that the SEW propagation length is directly proportional to the real part and inversely proportional to the imaginary part of the permittivity

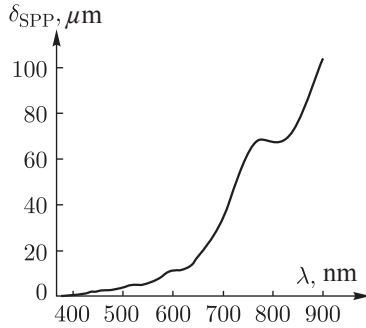


**Fig. 4.2.4.** Dependence of the length distribution of the SEW on the wavelength.

of the metal. Figure 4.2.4 shows the length distribution of the SEW (4.2.151) on the wavelength of light for the given pair of materials. The graph shows that when the value of the wavelength approaches the resonant value  $\lambda > 368$  nm the propagation length tends to zero. The practical use of the SEW is impossible in the vicinity of the resonance wavelength.

The penetration depth of the SEW into the medium is defined as the distance at which the wave amplitude decreases by  $e$  times. According to (4.2.129)–(4.2.131), (4.2.136), the damping of the SEW is determined by the

$$k_{z,l} = k_0 \gamma_l = \sqrt{k_{\text{SPP}}^2 - \varepsilon_l k_0^2}, \quad (4.2.156)$$

where the superscript  $l$  denotes the metallic ( $m$ ) or dielectric ( $d$ ) environment. The depth of penetration takes the form

$$\delta_l = 1 / \left| \operatorname{Re}(k_{z,l}) \right|. \quad (4.2.157)$$

When the condition (2.4.144) is fulfilled, the following approximate expressions hold:

$$\delta_d \approx \frac{1}{k_0} \left| \frac{\varepsilon'_m + \varepsilon_d}{\varepsilon_d^2} \right|^{\frac{1}{2}}, \quad (4.2.158)$$

$$\delta_m \approx \frac{1}{k_0} \left| \frac{\varepsilon'_m + \varepsilon_d}{(\varepsilon'_m)^2} \right|^{\frac{1}{2}}. \quad (4.2.159)$$

These formulas for the penetration depths  $\delta_d, \delta_m$  are of practical importance, since they allow to determine the minimum thickness of material required for the excitation and existence of SEW. Figures 4.2.5 and 4.2.6 show the dependences of the depth of penetration of the SEW in the dielectric and the metal environment on

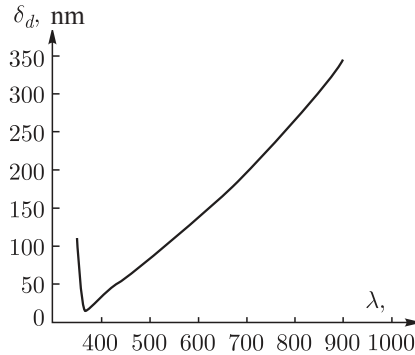


**Fig. 4.2.5.** The dependence of the penetration depth of SEW in a dielectric medium on the wavelength.

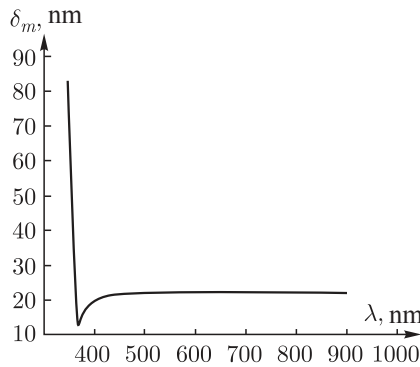


**Fig. 4.2.6.** The dependence of the penetration depth of SEW in the metal environment on the wavelength.

the wavelength. It is seen that for values of the wavelength far from the resonance value, the penetration depth of SEW in the metal environment is similar to a constant value equal to 22 nm.

#### 4.2.1.3. Excitation of surface electromagnetic waves

One of the most common schemes used for the formation of the SEW is the Kretschmann scheme [32–38]. The Kretschmann scheme includes a glass prism with a metal foil at the bottom (Fig. 4.2.7a). The film material is represented by good electrical conductors (silver, gold). At a certain angle of incidence of the wave with TM-polarization from the side of the prism SEWs are excited at the lower boundary of the metal film [32–38]. The diagram in Fig. 4.2.7a is described by the model of the three-layer medium in Fig. 4.2.7b. The dielectric constants 1–3 in

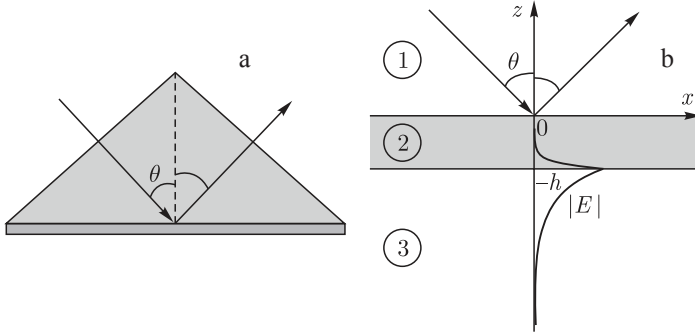


**Fig. 4.2.7.** Diagram of SEW excitation (a) and the equivalent model (b).

Fig. 4.2.7b correspond to the materials of the prism ( $\varepsilon_{pr}$ ), the metal layer ( $\varepsilon_m$ ) and the substrate ( $\varepsilon_d$ ).

SEW excitation occurs at an angle of incidence  $\theta$ , defined by the condition of equality of the projection of the wave vector of the incident wave to the direction of propagation of SEW (axis  $Ox$ ) to the propagation constant of SEW. This condition has the form

$$k_{x,0} = k_0 \sqrt{\varepsilon_{pr}} \sin \theta = \text{Re}(k_{\text{SPP}}). \quad (4.2.160)$$

Condition (4.2.160) is approximate. This is due to the fact that formula (4.2.137) defines the propagation constant of SEW for the boundary of semi-infinite media, and the metal film in Fig. 4.2.7 has a finite thickness. In practice, the film thickness is 40–50 nm. The error of determining the angle  $\theta$  from the formula (4.2.160) is about  $0.1^\circ$  and in most practical problems is not essential. The exact definition of the angle  $\theta$  is to solve the problem of diffraction of a plane wave with TM-polarization on a homogeneous metal layer. The SEW excitation angle is determined by a sharp minimum that appears in the reflection spectrum of excitation of the SEW. Figure 4.2.8 shows a typical plot of the reflection coefficient  $R(\theta)$  calculated with the following parameters:  $\lambda = 550$  nm,  $h = 50$  nm,  $\varepsilon_{pr} = 4$ ,  $\varepsilon_m = -12.922 + 0.447i$  (Ag),  $\varepsilon_d = 2.25$ .

With these parameters, the surface wave excitation occurs at an angle of incidence  $\theta_{\text{SPP}} = 63.18^\circ$ . Note that the angle obtained from (4.2.160) is in this case  $\theta_{\text{SPP}} = 63.28^\circ$ .

Consider in the model of SEW excitation (Fig. 4.2.7) not one but two symmetrically incident TM-waves:

$$H_{0y}^{(1)}(x, z) = \exp\left(ik_{x,0}x - ik_z^{(1)}z\right) + \exp\left(-ik_{x,0}x - ik_z^{(1)}z\right), \quad (4.2.161)$$

where  $(k_z^{(1)})^2 = k_0^2 \varepsilon_{pr} - k_{x,0}^2$ . In this case, two SEWs propagating in opposite directions will be excited along the boundary of zones 2 and 3. As a result, the interference pattern of the SEW will form directly under the metal film. From Maxwell's equations we can easily obtain the distribution of the electric field intensity

( $|\mathbf{E}|^2 = |E_x|^2 + |E_z|^2$ ) under the film (when  $z \leq -h$ ) in the form

$$|\mathbf{E}_{\text{SPP}}(x, z)|^2 \sim \left( \left( k_{x,0}^2 - |k_z^{(3)}|^2 \right) \sin^2(k_{x,0}x) + |k_z^{(3)}|^2 \right) \exp\left(2|k_z^{(3)}|(z+h)\right), \quad (4.2.162)$$

where  $(k_z^{(3)})^2 = k_0^2 \varepsilon_d - k_{x,0}^2$ . Equation (4.2.162) describes the interference pattern periodic with respect to the axis  $Ox$  and exponentially decaying along the axis  $Oz$ . The period of the interference pattern is the same as the function  $\sin^2(k_{x,0}x)$ , i.e.

$$d_{\text{ip}} = \frac{\pi}{k_{x,0}} = \frac{\pi}{\text{Re}(k_{\text{SPP}})} = \frac{\lambda}{2\sqrt{\varepsilon_{\text{pr}}} \sin \theta_{\text{SPP}}}, \quad (4.2.163)$$

where  $\theta_{\text{SPP}}$  is the angle of incidence, defined by the condition (4.2.160).

The contrast of the interference pattern is given by

$$K = \frac{\max_x \left\{ |\mathbf{E}_{\text{SPP}}(x, -h)|^2 \right\} - \min_x \left\{ |\mathbf{E}_{\text{SPP}}(x, -h)|^2 \right\}}{\max_x \left\{ |\mathbf{E}_{\text{SPP}}(x, -h)|^2 \right\} + \min_x \left\{ |\mathbf{E}_{\text{SPP}}(x, -h)|^2 \right\}}. \quad (4.2.164)$$

When the condition (2.4.21) is fulfilled, the following simple expression can be obtained for contrast:

$$K = \frac{|k_{x,0}|^2 - |k_z^{(3)}|^2}{|k_{x,0}|^2 + |k_z^{(3)}|^2} \approx 1 - \frac{2\varepsilon_d}{|\varepsilon_m'| + \varepsilon_d}. \quad (4.2.165)$$

If a photorecording material is placed in the area under the metal film, the interference pattern of the SEW can be written and used for making a diffraction grating with period  $d_{\text{ip}}$ . The width of the step is controlled by exposure time.

Practical use of the considered scheme for the formation of interference patterns of the SEW is inconvenient for several reasons. In particular, two coherent beams are required, the scheme is not compact, and the formation of an interference pattern in a dense dielectric medium requires a prism made of a material with high dielectric constant, etc.

### 4.2.2. Formation of one-dimensional interference patterns of surface electromagnetic waves

Consider the formation of one-dimensional interference patterns of SEW with a diffraction structure consisting of a binary dielectric diffraction grating and a metallic film below the grating [21–24]. The geometry of the structure shown in Fig. 4.2.9. Above and below the structure there is a homogeneous dielectric with refractive indices  $n_1$  and  $n_{11}$ , respectively. At the period  $d$  the grating has a single